remote sensing

MDPI

Article

Satellite-Based Assessment of Rocket Launch and Coastal Change Impacts on Cape Canaveral Barrier Island, Florida, USA

Hyun Jung Cho [1], Daniel Burow [2], Kelly M. San Antonio [1], Matthew J. McCarthy [3,*], Hannah V. Herrero [4], Yao Zhou [2], Stephen C. Medeiros [5], Calvin D. Colbert, Jr. [6] and Craig M. Jones [6]

1 Department of Integrated Environmental Science, Bethune-Cookman University, 640 Dr. Mary McLeod Bethune Blvd, Daytona Beach, FL 32114, USA; choh@cookman.edu (H.J.C.)
2 Meteorology Program, Applied Aviation Sciences Department, Embry-Riddle Aeronautical University, 1 Aerospace Boulevard, Daytona Beach, FL 32114, USA; burowd@erau.edu (D.B.); zhouy12@erau.edu (Y.Z.)
3 Remote Sensing Group, Oak Ridge National Laboratory, Geospatial Science and Human Security Division, UT-Battelle, 1 Bethel Valley Road, Oak Ridge, TN 37830, USA
4 Department of Geography & Sustainability, University of Tennessee, 1000 Philip Fulmer Way, Knoxville, TN 37996-0925, USA; hherrero@utk.edu
5 Department of Civil Engineering, Embry-Riddle Aeronautical University, 1 Aerospace Boulevard, Daytona Beach, FL 32114, USA; medeiros@erau.edu
6 National Geospatial-Intelligence Agency, 7500 GEOINT Dr., Springfield, VA 22150, USA; calvin.d.colbert@nga.mil (C.D.C.J.); craig.m.jones@nga.mil (C.M.J.)
* Correspondence: mccarthymj@ornl.gov

Abstract: The Cape Canaveral Barrier Island, home to the National Aeronautics and Space Administration (NASA)'s Kennedy Space Center and the United States (U.S.) Space Force's Cape Canaveral Space Force Station, is situated in a unique ecological transition zone that supports diverse wildlife. This study evaluates the recent changes in vegetation cover (2016–2023) and dune elevation (2007–2017) within the Cape Canaveral Barrier Island using high-resolution optical satellite and light detection and ranging (LiDAR) data. The study period was chosen to depict the time period of a recent increase in rocket launches. The study objectives include assessing changes in vegetation communities, identifying detectable impacts of liquid propellant launches on nearby vegetation, and evaluating dune elevation and tide level shifts near launchpads. The results indicate vegetation cover changes, including mangrove expansion in wetland areas and the conversion of coastal strands to denser scrubs and hardwood forests, which were likely influenced by mild winters and fire management. While detectable impacts of rocket launches on nearby vegetation were observed, they were less severe than those caused by solid rocket motors. Compounding challenges, such as rising tide levels, beach erosion, and wetland loss, potentially threaten the resilience of launch operations and the surrounding habitats. The volume and scale of launches continue to increase, and a balance between space exploration and ecological conservation is required in this biodiverse region. This study focuses on the assessment of barrier islands' shorelines.

Keywords: Cape Canaveral Barrier Island complex; Florida central east coast; coastal vegetation; NDVI; LiDAR; rocket launch; Kennedy Space Center; Cape Canaveral Space Force Station; SpaceX

check for updates

Citation: Cho, H.J.; Burow, D.; San Antonio, K.M.; McCarthy, M.J.; Herrero, H.V.; Zhou, Y.; Medeiros, S.C.; Colbert, C.D., Jr.; Jones, C.M. Satellite-Based Assessment of Rocket Launch and Coastal Change Impacts on Cape Canaveral Barrier Island, Florida, USA. *Remote Sens.* **2024**, *16*, 4421. https://doi.org/10.3390/rs16234421

Academic Editor: Javier Marcello

Received: 1 October 2024
Revised: 8 November 2024
Accepted: 20 November 2024
Published: 26 November 2024

Copyright: © 2024 by the authors. Licensee MDPI, Basel, Switzerland. This article is an open access article distributed under the terms and conditions of the Creative Commons Attribution (CC BY) license (https://creativecommons.org/licenses/by/4.0/).

1. Introduction

Florida's barrier island systems are under increasing pressure from natural and anthropogenic forces [1,2]. Climate change increasingly exacerbates the impacts of natural disturbances, including coastal storms, sea-level rise (SLR), and erosion [3,4]. Human activities such as development, pollution, and coastal armoring contribute to habitat destruction and conversion [5,6].

The Cape Canaveral Barrier Island on the east central coast of Florida (Figure 1) houses the National Aeronautics and Space Administration (NASA)'s Kennedy Space Center (KSC) and the United States Space Force (USSF)'s Cape Canaveral Space Force

Station (CCSFS). These facilities are adjacent to the United States Fish & Wildlife Service's Merritt Island National Wildlife Refuge (MINWR) and the U.S. National Park Service's Canaveral National Seashore (CANA). The area supports some of the richest wildlife diversity among federal facilities in the continental United States due to its unique positioning at the transition zone between the temperate Carolinian and sub-tropical Caribbean zoogeographic provinces [3]. The space industry contributes significantly to Florida's economy; the 2021 KSC's Fiscal Year report estimated its annual economic output in Florida to be $5.25 billion (https://www.nasa.gov/general/nasa-generates-billions-in-economic-impact-for-florida-space-coast/ (accessed on 1 August 2024)).

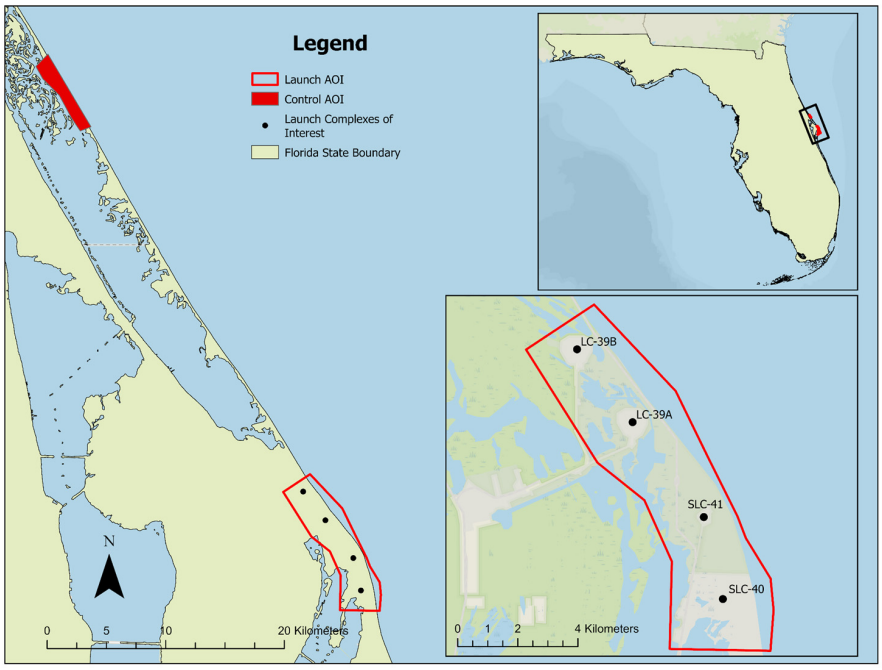

Figure 1. The study location includes the launch AOI (open red polygon) within the Cape Canaveral Barrier Island and the control AOI (closed red polygon) within the Canaveral National Seashore (CANA), Florida. The study location is within east central Florida (upper right inset). The launch AOI contains the four launchpads of interest (Launch Complexes 39B, 39A, 41, and 40 from north to south) and is indicated within an open red polygon (lower right inset). AOI stands for area of interest.

The land elevation range of the Cape Canaveral Barrier Island was estimated to be from sea level to nine meters, with a mean land elevation of 1.05 m above the mean lower high water (MLHW) [3]. The estimated mean elevation was highest in oak scrub (1.96 ± 1.65 m) and lowest in saltmarsh (0.14 ± 0.55 m), with there being significant overlap observed among vegetation communities [3].

Besides the chronic stresses of SLR, this region faces an increasing frequency and intensity of pulse disturbances such as hurricanes and rocket launches. Rising global temperatures are linked to more frequent and intense heat waves and altered precipitation patterns, impacting local ecosystems and water resources [7,8]. The increasing intensity of hurricanes, driven by warmer sea-surface temperatures, enforces a substantial threat to the region, with more powerful storms leading to severe storm surges and flooding [9]. Sea-level rise also contributes to saltwater intrusion into freshwater habitats and aquifers [10]. Cape Canaveral Barrier Island's low-lying geography makes the KSC and CCSFS particularly vulnerable to these risks [3,11], meaning that resilience measures are required to safeguard space launch activities.

Several environmental alterations and management strategies have been implemented in the area. These include the construction of mosquito control impoundments in the 1950s

and 1960s to reduce the prevalence of disease-carrying mosquitoes during the construction of the KSC, which has altered the natural hydrology of estuarine wetlands in the area [12]. Fire suppression, a type of fire management, reduced the habitat suitability of the scrub ecosystems and scrub-dependent species on the island [13]. Prescribed fire (also known as controlled burn) programs, administered to restore the natural fire regimes essential for maintaining fire-adapted ecosystems such as scrub and pine flatwoods and to prevent the accumulation of fuels for wildfire, can alter plant composition and dominance [14]. Additionally, beach nourishment projects are conducted at locations where coastal erosion threatens safe launchpad operation, and dune restoration efforts are carried out which focus on rebuilding and stabilizing dunes to protect against storm surges and SLR [15,16].

Foster et al., 2017 [3], investigated how hydrological changes would affect the coastal vegetation community of the Cape Canaveral Barrier Island using three SLR scenarios. Their model predicted decreases in coastal upland communities (scrub-shrub) and increases in salt marshes under a 0.2 m SLR increase scenario. Much of the coastal uplands (pine flatwoods, scrubs, hardwood hammocks) were predicted to be converted to mangrove wetlands or invaded by non-native plants that are tolerant to flooding, fire, and saltwater [3,11]. In these regions, the previous areas of salt marshes (coastal wetlands dominated by herbaceous plants) have been replaced with mangroves due to the northward migration of mangroves resulting from the reduced frequency of days with freezing air temperatures [17].

The topography, hydrologic systems, and plant community in this area are shaped by and evolve with a combination of sharp pulse disturbances, such as hurricanes, rocket launches, and fires, alongside chronic stressors like SLR, global warming, and fire suppression. Additionally, rapid-onset events, such as construction and modifications to launch facilities, further contribute to these complex and interconnected effects. Many coastal ecosystems demonstrate resilience to short-term extreme events like hurricanes, floods, and storm surges [18]. However, their long-term resilience and the ability of the communities to adapt to the rapidly accelerating changes in sea level, rocket launches, and warming temperatures remains unknown.

The environmental impact of rocket emissions varies greatly with the size and type of rockets, the launch time and frequency, the emission altitude, the local atmospheric and environmental conditions, and the type of propellant used. Both solid and liquid propellants are in use, each producing different emission products [19]. The fuels used for solid rocket motors (SRMs) have been of particular concern due to them including compounds like hydrochloric acid (HCl) and alumina particles.

The environmental impact studies of rocket launches have primarily focused on solid rocket propellants and on cases of singular launches or a small number (less than five) of annual launches, with stratospheric ozone depletion as their environmental focus [20]. Previous studies [11,21–24] have documented the environmental impacts of solid rocket motor-based launches from the KSC and CCSFS. Ground-based surveys and the rocket exhaust effluent diffusion (REED) model were used to document the acute effects of individual launches and to estimate the cumulative effects of repeated launches. The ground cloud, formed from the interaction of exhaust from solid rocket boosters with deluge water, leads to vegetation changes resulting from the repeated near-field deposition of aluminum oxide and hydrochloric acid. Previously observed damages to plants after launches also include tree uprooting, broken branches, and leaves scorched from heat and flame [21].

Thus far, there is a lack of studies conducted to assess the potential impacts of the increasing numbers of launches of the Falcon 9 rockets that use liquid oxygen (LOx) and rocket-grade kerosene (RP-1) propellant. The byproducts of these are mainly water and carbon dioxide, the environmental impact of which is deemed to be low compared to the solid rocket motor exhaust products. As the space industry increases the frequency of shuttle launches, particularly from locations like Cape Canaveral Barrier Island, it is critical to document the potential cumulative impacts of launches.

This study evaluates the recent changes in vegetation cover (2016–2023) and dune elevation (2007–2017) within the Cape Canaveral Barrier Island using high-resolution optical satellite and light detection and ranging (LiDAR) data. The study period was chosen to depict the time period of a recent increase in rocket launches from the KSC and CCSFS launches (e.g., from 5 launches in 2016 to 55 in 2023 at the CCSFS' Space Launch Complex 40). Due to the limited LiDAR data for recent years available for this location, the dune elevation was compared within the period from 2006/2007 to 2016/2017. The study questions to address are whether: (1) there have been changes in the coastal vegetation community as predicted by previous studies (coastal upland habitat conversion to wetlands and saltmarsh conversion to mangroves); (2) the impacts of rocket launches using the liquid propellant on nearby vegetation are detectable; and (3) there were changes in dune elevation and the tide level near the launchpads. The results of this study were used to convey potential impacts of the area's changes in vegetation cover and elevation on the resilience of the barrier island system, including launch operations, particularly at the Launch Complex 39A, which is being proposed to be modified to accommodate the Starship-Super Heavy vehicle launch operation and booster landing.

2. Materials and Methods

2.1. Study Area

The study area spans a northern section of the Cape Canaveral Barrier Island (Figure 1). The launch study area is ~37 km^2 (Figure 1). The KSC's Launch Complex 39A (LC-39A) and CCSFS's Space Launch Complex 40 (SLC-40) have been leased to and heavily utilized by Space Exploration Technologies Corporation (SpaceX) for its Falcon 9 rocket launches. SLC-40 has been a primary site for SpaceX rocket launches after its repair following a catastrophic accident during a routine pre-launch static fire test on 1 September 2016. LC-39A, originally used for Apollo and Space Shuttle missions, has been used and managed by SpaceX since February 2017 (with a total of 95 launches between 2017 and 2023). The nearby launchpads, LC-39B and SLC-41, have comparable sizes and configurations to LC-39A and SLC-40, respectively, but are used infrequently. LC-39B had previously not been used for launches since 2009, until the Artemis 1 launch on 16 November 2022.

The KSC's coastlines are impacted by frequent storm surges, compounded by sea-level rise exceeding 12.7 cm from 1995 to 2015 [3,16]. The Florida Department of Environmental Protection categorized the area as "critically eroded", indicating that a threat to habitats for several protected wildlife species with the loss of primary and secondary dunes and adjacent coastal habitats [16]. To address increasing erosion risks, NASA implemented an adaptive management strategy in 2010 and 2013/2014, creating two dunes totaling 1.7 km in length near LC-39A and LC-39B to facilitate managed restoration while protecting national assets and providing additional wildlife habitat [16]. The most recent dune restoration was completed in 2019/2020 after damages by Hurricane Matthew in October 2016 (*Personal communication*: Tammy Foster [25]).

2.2. Land Cover Change Surrounding the Heavily Used Launch Pads

WorldView (WV) multispectral images were used to investigate vegetation cover changes from 2016 to 2023 at the Cape Canaveral launch site (launch AOI in Figure 1) and also at the Canaveral National Seashore (CANA) control site (control AOI in Figure 1; ~6 km^2). The control site is a barrier island area, influenced by natural stresses and disturbances comparable to those of the Cape Canaveral launch site. The control site was chosen to serve as a reference for land cover and dune elevation with minimal manmade infrastructures because it is under the National Park Service's jurisdiction.

Level-1B WorldView-2 and WorldView-3 (WV-2 and WV-3) images that cover the launch AOI and control AOI (cloud cover < 20% with clear views of the launchpads) were acquired (https://evwhs.digitalglobe.com/ (accessed on 7 July 2024 and 1 August 2024); the Global Enhanced Geoint Delivery (G-EGD) portal). The 2 m spatial resolution, multispectral WV images were orthorectified, radiometrically calibrated, and then atmospherically

corrected using Py6S, which is a Python wrapper for the robust Second Simulation of the Satellite Signal in the Solar Spectrum (6S) model. The 6S model was implemented to atmospherically correct WorldView spectral bands by accounting for viewing geometry (i.e., sun/sensor azimuth and zenith angles), Earth–Sun distance, sensor and target altitude, dominant aerosol types, water vapor, and ozone.

The images from October 2016 (8 October 2016 for launch AOI; 30 October 2016 for control AOI), August 2023 (4 August 2023, for launch AOI), and December 2023 (19 December 2023 for control AOI) were used to produce land cover classification maps. The study area is within the Humid Subtropical Climate region (Cfa) according to the Köppen classification [26]. Cape Canaveral experiences seasonal rainfall variations, averaging 5.1–7.6 cm per month in winter (November–April) and 15.3–17.8 cm in summer (June–September), with May and October as transition periods [27]. Pixels covering the Atlantic Ocean and clouds were masked from the images.

The support vector machine (SVM) machine-learning algorithm [28] was used to classify each of the images into seven classes (water, clear-cuts/lawns, impervious surfaces/bare sand, two coastal upland vegetation classes, and two coastal wetland classes; Table 1). Foredunes are located closest to the ocean and act as the first line of defense against storms and erosion, supporting pioneer species of herbaceous vegetation. Coastal strands, characterized by sandy soils and salt-tolerant plants, form just inland from the foredunes. Coastal scrub habitats feature shrubby vegetation thriving in well-drained sandy soils, providing important habitats for the Florida endemic scrub jays (*Aphelocoma coerulescens*), the threatened eastern indigo snakes (*Drymarchon couperi*), and the keystone species gopher tortoises (*Gopherus polyphemus*). Maritime hammocks, more sheltered and humid, are hardwood forests. Mangroves, found in tidal estuarine shores, are vital for stabilizing shorelines and providing nurseries for marine life, while coastal salt marshes, dominated by grasses and rushes, serve as buffers between land and water, filtering pollutants while also absorbing floodwaters and kinetic storm energy. Together, these ecosystems create a mosaic of land covers that sustains Florida's coastal biodiversity [29–32].

Table 1. Land cover classes defined for support vector machine (SVM) machine-learning algorithm. The class names assigned to the classes and their respective National Vegetation Classifications (NVCs) are indicated based on the NVC Standard by the Federal Geographic Data Committee (FGDC; Document number: FGDC-STD-005-2008).

Land Cover Class	Class Name	NVC Standard	Dominant Land Cover and Plants
Water	Water	NA	Estuarine waters and impounded area
Impervious surface/Sand	Impervious/Sand	NA	Constructed areas including launchpads and roads
Clear-cut/Lawn	Clearcut/Lawn	Developed vegetation	Mowed vegetation and turfgrass
Foredune/Coastal strand	Foredune/Strand	Shrubland (dwarf) and Grassland	Sea oats, beach sunflower, sea purslanes, saw palmetto, sea grape; salt-tolerant plants
Coastal Scrub/Maritime Hammock	Scrub/Hammock	Shrublands (tall) and Forest	Sand pines, oaks, cabbage palms, red cedars; hardwood and palms
Mangrove Swamp	Mangroves	Forested Wetland	Black, red, and white mangroves
Coastal Saltmarsh	Coastal Marsh	Herbaceous Wetland	Cordgrasses, rushes, and sedges

The community changes in species composition and dominance across the coastal upland habitats, from foredunes, coastal strands, and coastal scrubs to maritime hammocks, are gradual, with several overlapping species. Therefore, the upland coastal classes were grouped into two classes: foredune/strands and scrubs/hammocks. Mangroves and salt marshes are the two wetland vegetation classes. Impervious surfaces (e.g., launchpads and roads) were grouped together with bare sand (e.g., sandy beaches) due to the spectral resemblance (Table 1).

Ground validation points were collected using the 2016, 2017, 2019, and 2022 aerial imagery accessed from the web map layers for Cape Canaveral Space Force Station (https://www.arcgis.com/home/item.html?id=78ea631a332445d183a16a443ea1f0e9 (accessed on 3 August 2024)), and ground-surveyed vegetation transect data (2016 through 2021) provided by NASA (for launch AOI) and authors (2016–2024; for Control AOI). The ground validation points were further supplemented by Google Earth (ver. 7.3 Google LLC) and interpreted by an author skilled in and familiar with the region's coastal plants and habitats. Between 100 and 140 points were collected for each class of each type of imagery; 75% of the points were used to train the classifier and the rest were used for validation.

To examine hot spots of land cover change, pixels that exhibited change between 2016 and 2023 according to the SVM analysis were coded with a value of 1, and pixels that did not exhibit land cover change were coded with a value of 0. Then, this binary land cover change raster was analyzed using the Getis-Ord Gi* tool in ArcGIS Pro (Version 3.1.3, Environmental Systems Research Institute, Inc.). This method uses z-scores and *p*-values to identify statistically significant spatial clusters of high (hot spots) and low (cold spots) values in a dataset, highlighting areas of significant clustering of land cover change and significant clustering of stable land cover.

A Normalized Difference Vegetation Index (NDVI) [33] was mapped for all available WV images acquired between October 2016 and December 2023. Mean NDVI values were calculated for each of the coastal upland (foredune/strand; scrub/hammock) and wetland classes (mangroves; coastal marsh) to determine if any substantial seasonality needed to be considered in comparing images obtained from different months.

2.3. Impacts of Individual Launch on Vegetation

There were four Falcon Heavy rocket launches that occurred from LC-39A in 2023. The Falcon Heavy combines three Falcon 9 boosters, making it a much larger and more powerful rocket. In order to document any changes in vegetation that can be attributed to Falcon Heavy launches, two launch dates (28 July 2023 and 28 December 2023) were selected. This study used PlanetScope imagery because there were more clear images available near the target launch dates compared to the WV imagery. The PlanetScope images were searched for those captured pre-launch (the imagery available before the launches), post-launch (within two days after the launches), and approximately 4 to 5 weeks after the launches. The dates of the obtained imagery are indicated in Table 2.

Table 2. Dates of the PlanetScope imagery used for pre-launch, post-launch, and one month after the three Falcon Heavy rocket launches from Launch Complex 39A of Kennedy Space Center. Wind direction and speed near the time of the launches were obtained from the nearby Automated Surface Observing Systems (ASOSs) stations (−80.5668; 28.4677).

Launch Date (Wind Direction and Speed)	28 July 2023 at 11:04 pm (S/SE, 3 knots)	28 December2023 at 8:07 pm (0 knot)
Pre-launch Image	23 July 2023	18 December 2023
Post-launch Image	30 July 2023	31 December 2023
One Month After	3 September 2023	31 January 2024

PlanetScope 3 m spatial resolution imagery was searched for images that were mostly cloud-free over the launch pads (LC-39A and LC-39B) and these were downloaded from the Planet imagery hub (https://www.planet.com/ (accessed on 1 August 2024)). These scenes were orthorectified and atmospherically corrected by Planet and represent surface reflectance. NDVI was calculated as an index for vegetation health and density. Areas with NDVI values greater than 0.2 in the 2016 map were selected to exclude non-vegetated surfaces. Change in vegetation health was calculated by subtracting the post-launch NDVI from pre-launch NDVI values.

Meteorological data (wind direction and speed) during each of the launch times were obtained from the nearby Automated Surface Observing Systems (ASOSs) stations to document potential factors that would affect the moving direction and extent of the fuel exhaust (steam and carbon dioxide) and other debris produced by selected launches.

2.4. Dune Elevation Changes

In order to compare the dune elevation changes near the launchpads with those near the control site in CANA, LiDAR data were downloaded from the National Oceanic & Atmospheric Administration (NOAA) Digital Coast (https://coast.noaa.gov/digitalcoast/; accessed on 1 August 2024). Table 3 below lists the LiDAR datasets along with their associated site and key metadata: average ground point density (GPD) and 95% confidence vertical position accuracy.

Table 3. LiDAR datasets used for elevation change analysis. Key metadata values for each dataset are nominal pulse density (NPD) and 95% confidence vertical position accuracy (non-vegetated terrain). NR stands for "Not Reported" and indicates that these values were not included in the metadata or accompanying report associated with a dataset.

Acquisition Date Range	Data Set Name	Site	NPD (Points/m^2)	95% Confidence Vertical Position Accuracy (cm)
2006	2006 Volusia County Florida LiDAR	Control	1	18.28
2007	2007 Florida Division of Emergency Management (FDEM) LiDAR Project: Brevard County	Launch	4	15
2010	2010 USACE NCMP Topobathy LiDAR: Atlantic Coast (NC, SC, GA, FL)	Both	NR	17.2
2016	2016 USACE NCMP Topobathy LiDAR DEM: Florida East Coast	Control	NR	9.5
2017	2017 USACE FEMA Topobathy LiDAR DEM: Florida East Coast, Florida Keys, and Collier County (Post Hurricane Irma)	Launch	NR	NR
2018	2018–2020 USGS LiDAR: Florida Peninsular FDEM—Brevard County	Launch	10.1	11.28
2018	2018–2020 USGS LiDAR: Florida Peninsular FDEM—Volusia County	Control	10.47	11.28

The LiDAR data were clipped and co-registered to the areas that all collections had in common for each site. This resulted in relatively narrow strips of the beaches along the Atlantic Ocean. The mean elevations and standard deviations were computed for the datasets and plotted over time to broadly compare the elevation trends at each site.

Four locations (CANA control site, LC-39A/B—in between 39A and 39B, LC-39A dune restoration site, and SLC-40/41) were selected for more detailed analysis. At each of these locations, 15 transects, perpendicular to the beach shorelines, were drawn on the LiDAR images to obtain dune profiles. The transect profile data from the 15 transects were used to compare dune elevation between 2006 and 2016 for the control site and between 2007 and 2017 for LC-39A/B and SLC-40/41. The 2018 LiDAR data did not extend to include all locations and, therefore, were not used in this transect analysis. Separate two-tailed t-tests were used to compare elevation changes between the years at the given locations.

2.5. Ancillary Data on Water Level, Temperature, and Prescribed Burns

Changes in coastal habitats are closely linked to alterations in water levels [34]. In particular, changes in the mean lower low water (MLLW), the average of the lowest daily tides, can reshape coastal habitats and species distribution by altering the depth and duration of root zone saturation and salinity [35].

Monthly tide data were downloaded from the National Oceanic and Atmospheric Administration's (NOAA) Tide & Currents portal (tidesandcurrents.noaa.gov; accessed on 15 August 2024) for the Trident Pier, Port Canaveral, Florida station (ID 8721604) for the time period from January 2010 to December 2023 using the MLLW datum. One-way ANOVAs were used to compare value changes in each of the tide variables (MHHW, MHW, MSL, MTL, and MLLW) between 2010 and 2023. In addition, a regression analysis was used to test if there was a change in MLLW during the period from January 2010 to December 2023. The time period was selected to include the recent accelerated rate of SRL [36].

The annual rate of changes in mean sea level (MSL) was calculated from the dataset and used to predict future MSL changes. Predicted inundation surrounding LC-39A was delineated using the LiDAR-driven digital elevation data to visualize potential inundation of the launchpad solely due to water level change. Launch Complex 39A was used for the visualization because of the increases in its use for rocket launches and its proximity to shorelines of the lagoon and the ocean.

Additionally, temperature is an important factor to consider as it has a substantial impact on mangrove survival and health, with mangrove freeze tolerance varying by species [37]. Black mangroves (*Avicennia germinans*), the most cold-tolerant, can withstand mild freezes for about one to two days if temperatures remain above −4 °C. Red mangroves (*Rhizophora mangle*) are more sensitive and may suffer damage or die after just one night of hard frost, especially if temperatures drop below −2 °C. Prolonged exposure to freezing conditions, typically more than two to three days, can cause significant dieback or mortality for most mangrove species. As temperatures rise and the frequency of extreme cold events decreases, mangrove species are expanding into areas previously dominated by salt marshes. The northward expansion of mangroves is an indicator of the ecological impacts of climate change on coastal ecosystems [38]. In order to document the number of days of freezing conditions within the study location, air temperature data were collected from the Global Historical Climatology Network daily (GHCNd) station near the Kennedy Space Center (Merritt Island, FL, USA). The number of days when the daily minimum temperature dropped below 0 °C during the period from 2005 and 2023 was obtained. The time period was chosen to include the exceptionally cold winters of 2005 and 2010 that affected this region.

Fire suppression during the 1960s through the early 1980s led to potential fuel accumulation in the study area [39]. Since 1992, KSC and Merritt Island National Wildlife Refuge have used mechanical treatments and prescribed burning to restore scrub vegetation in order to improve the habitat for the Florida scrub-jay. Schmalzer and Adrian (2001) [40] found that long-unburned scrub grows faster than regularly burned areas, indicating the need for more frequent burns during restoration to maintain the habitat's suitability for scrub-dependent species. Data and shapefiles of the burn areas during the prescribed fires were obtained from the Monitoring Trends in Burn Severity (MTBS) website (mtbs.gov; accessed on 11 August 2024). The MTBS program, launched in 2005 by the US Forest Service and the Department of the Interior, maps the location, extent, and burn severity of all large fires in the United States.

3. Results

3.1. Land Cover Change Between 2016 and 2023

The 2016 and 2023 SVM classification maps of the control AOI (control AOI in Figure 1) are presented in Figure 2. The overall classification accuracy of the control AOI was 86.64% for 2016 (30 October 2016) and 74.34% for 2023 (23 January 2023). A substantial portion of the scrub/hammock was misclassified as mangroves, resulting in the user accuracy being a mere 21% in 2023, while the producer's accuracy was 92% for mangroves and 99% for scrub/hammock. Scrub/hammock was also misclassified as foredune/strand (user accuracy of 30%), while the producer's accuracy for foredune/strand was 84%. All other accuracies were between 80% and 100% for the control AOI. The prominent land cover changes between 2016 and 2023 at the control AOI included scrub/hammock conversion to

mangrove (10.27%) or to foredune/strand (8.1%), which appeared to be largely due to the misclassification. All other land cover changes accounted for less than 1%.

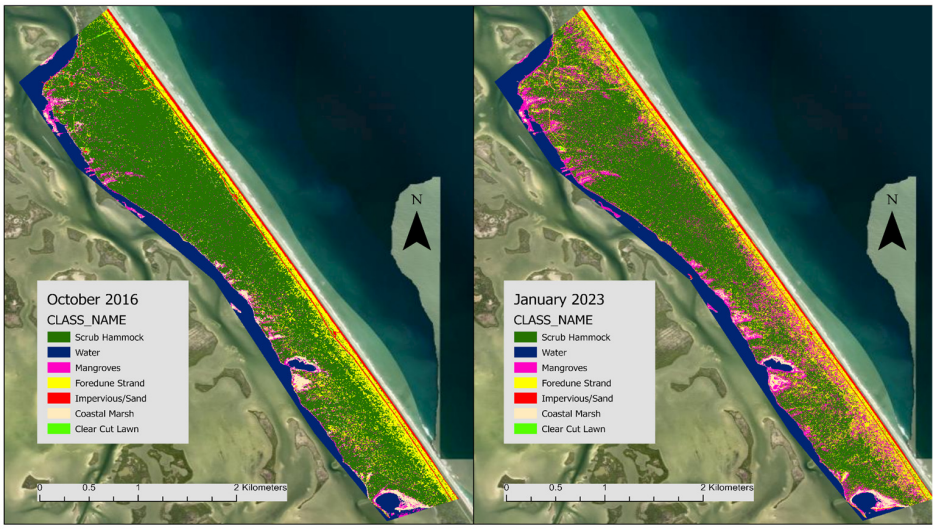

Figure 2. The 2016 and 2023 SVMs' (support vector machines') classification maps of the control site located within the Canaveral National Seashore, Florida. The WorldView imagery (copyright 2020 DigitalGlobe NextViewLicense) from 30 October 2016 and 11 January 2023 were used to produce the land cover classification maps.

The 2016 and 2023 SVM classification maps of the Cape Canaveral Barrier Island's launch site (launch AOI in Figure 1) are presented in Figure 3. The overall classification accuracy was 72.0% for 2016 and 83.9% for 2023. There were classification errors in correctly classifying foredune/strand from scrub/hammock or vice versa, representing 22% of the classifications. Distinction between mangrove and marsh also resulted in errors of 25%, and errors of 29% occurred when distinguishing shrub/hammock from mangrove.

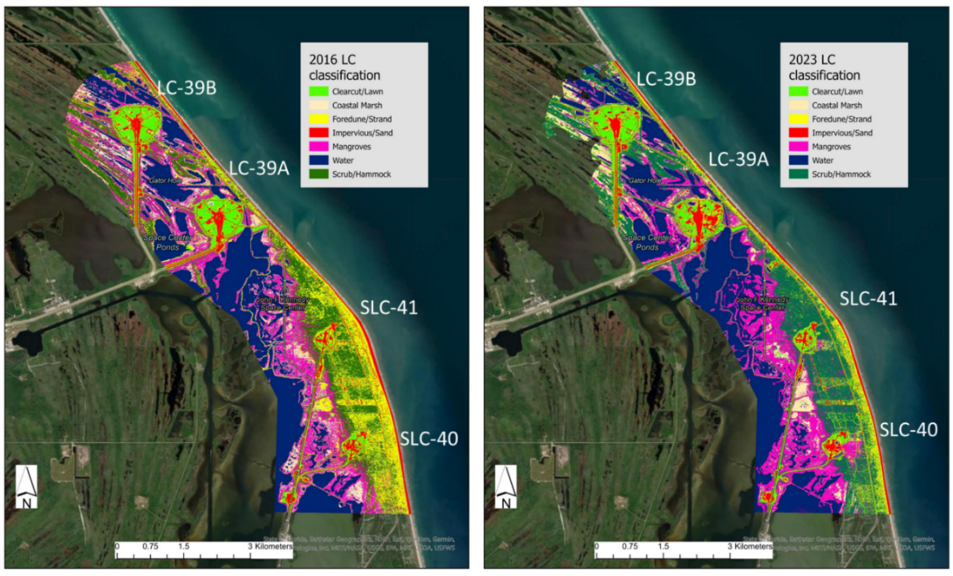

Figure 3. Land cover classification maps of the Cape Canaveral Barrier Island's launch site. The WorldView imagery (copyright 2020 DigitalGlobe NextViewLicense) from 8 October 2016 (**left**) and 4 August 2023 (**right**) was used to produce the land cover classification maps. The four launchpads are labeled: Launch Complex (LC)-39B, LC-39A, Space Launch Complexes (SLC)-41, and SLC-40 (top to bottom). The maps were created using ArcGIS software and ArcGIS Online basemap by ESRI (Copyright © Esri. All rights reserved).

In order to examine the similarity between the spectra of the misclassified vegetation classes, spectral profiles of the four natural vegetation cover classes (i.e., coastal marsh, mangroves, foredune/strand, and scrub/hammock) were derived from all pixels of the 2016 and 2023 WV images that correspond to the given classes. The mean reflectance at all bands for the four classes is presented in Figure 4.

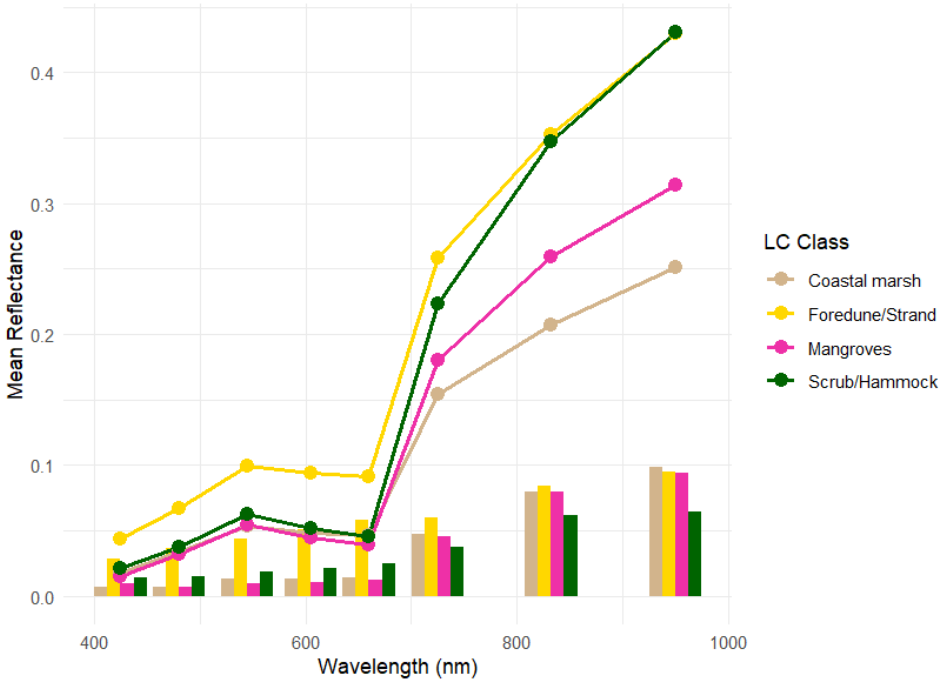

Figure 4. Spectral profiles of four vegetation classes: coastal marsh, mangroves, foredune/strand, and scrub/hammock. The spectral profiles are the mean reflectance values at the WorldView eight bands, calculated from the WorldView imagery of 8 October 2016 and 4 August 2023. Standard deviations within each band/class combination are displayed as bars below the lines.

The foredune/strand areas exhibit higher reflectance in the shorter wavelength range (bands 1–6; Figure 4), indicating a relatively sparse vegetation cover where sandy soil is visible through less dense vegetation. In contrast, the wetland classes display lower reflectance in the near-infrared spectrum (bands 6–8) due to water absorption in the background (Figure 4). Coastal marshes, primarily herbaceous, have lower reflectance than tree-dominated areas of mangroves or scrub/hammock. This study's scope concerns changes in vegetation type and cover (e.g., wetland vs. upland, herbaceous marsh vs. mangrove forest, open strand vs. closed hardwood forest) rather than achieving precise classification accuracy. As a result, the classification accuracy for the launch site was deemed acceptable for this purpose.

Three sub-sections were selected from the classification maps in Figure 3 to focus on the vicinities of LC-39B, LC-39A, and SLC-40/41 (Figure 5). In the area surrounding LC-39B, a noticeable portion of the mangrove areas seen in 2016 (top left in Figure 5) were converted to marshes or coastal upland in 2023, even with the cloud mask (top right in Figure 5). In the area surrounding LC-39A, there were considerable changes in the marsh-to-mangrove conversion and thinning of the coastal wetlands, resulting in the conversion of wetlands (marshes and mangroves) to open water (middle left and right in Figure 5). The wetlands-to-water conversions over time are also visualized in the color infrared images in Figure 6. Wetland loss near LC-39A is prominent along the dikes of the mosquito control impoundments shown in Figure 6. The noticeable vegetation cover changes surrounding SLC-40/41 are marsh conversion to mangrove in wetland areas and herbaceous/open shrubs conversion to hammocks (bottom left and right in Figure 5).

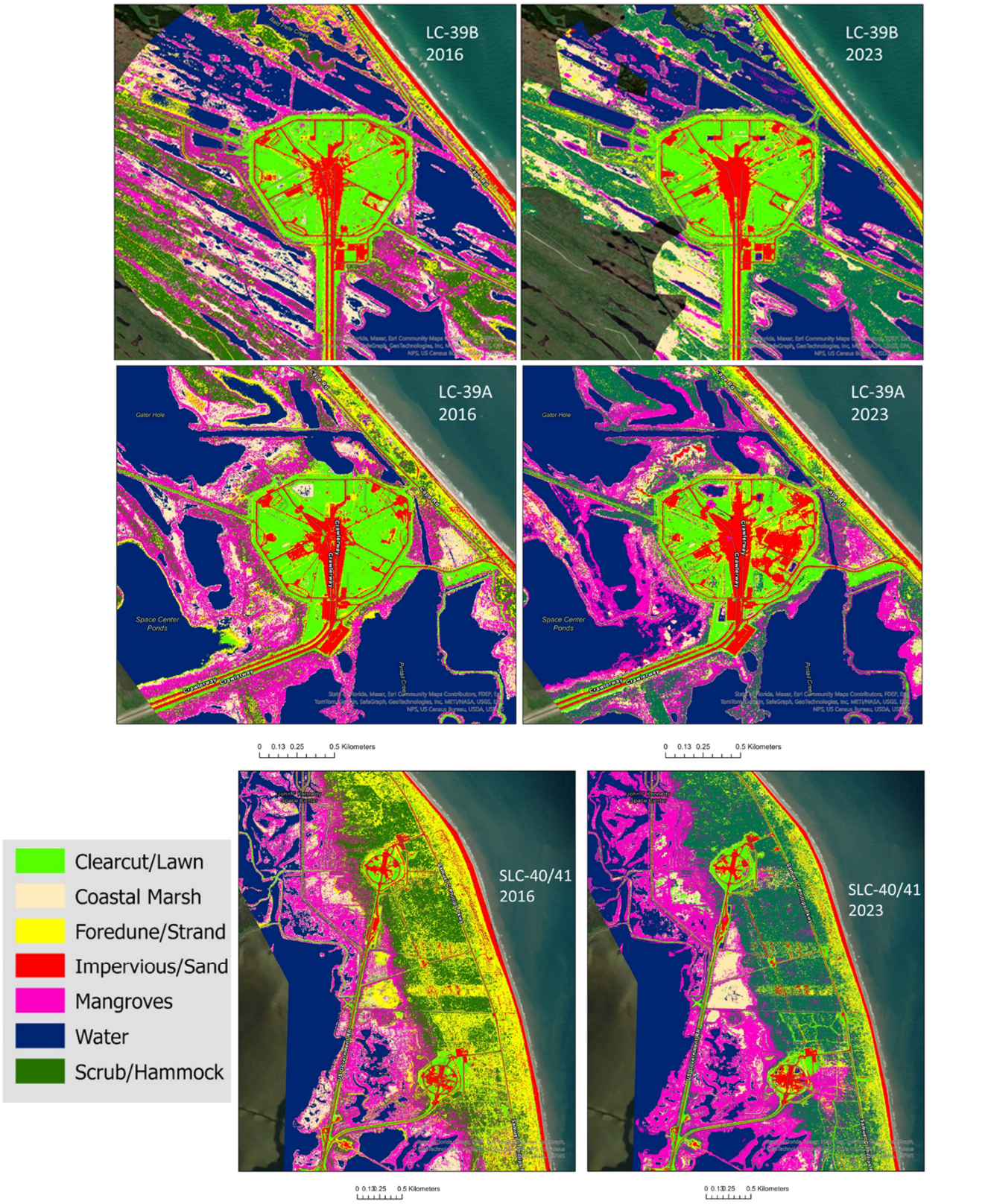

Figure 5. Land cover classification maps of the Cape Canaveral Barrier Island's launch site. The WorldView imagery (copyright 2020 DigitalGlobe NextViewLicense) from 8 October 2016 and 4 August 2023 were used to produce the land cover classification maps. Top to bottom panels: the vicinities of Launch Complex (LC) 39B, LC-39A, and Space Launch Complex (SLC)-41/40, respectively. The maps were created using ArcGIS software and ArcGIS Online basemap by ESRI (Copyright © Esri. All rights reserved).

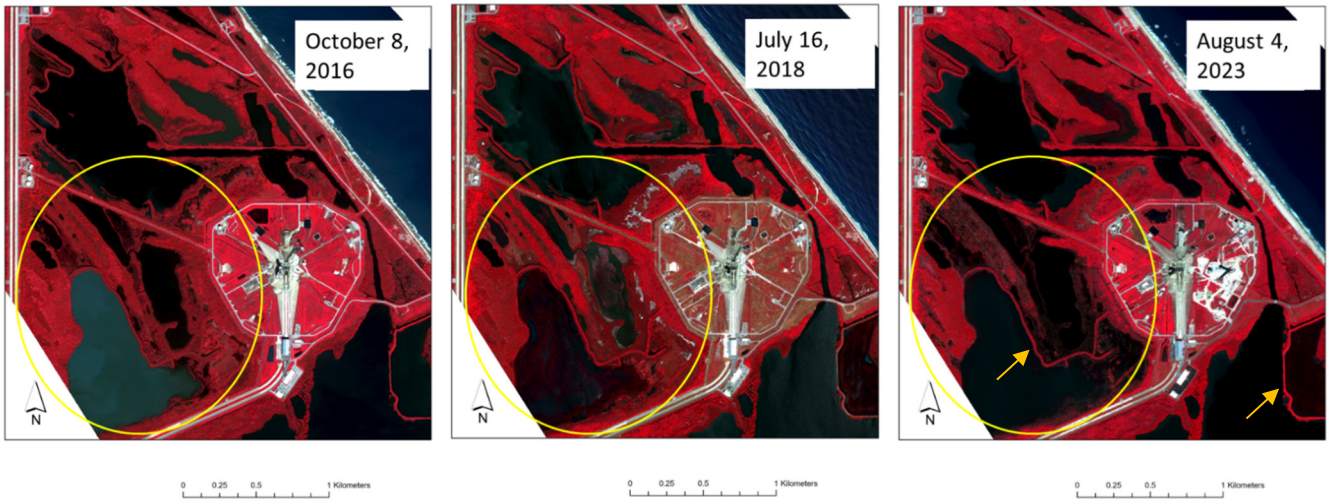

Figure 6. Color infrared displays of the WorldView imagery (Bands 7, 5, and 3, where band centers correspond to 833, 659, and 546 nm, respectively; copyright 2020 DigitalGlobe NextViewLicense) of 8 October 2016 (**left**), 16 July 2018 (**center**), and 4 August 2023 (**right**). The areas of marsh thinning from 2016 to 2023 are indicated with yellow open circles. The impounded areas for mosquito control are shown, which have limited hydrologic connection to the lagoon, as they are separated with dikes (indicated with yellow arrows). The seasonal water level in this region is highest in October and lowest between July and August. (https://psmsl.org/data/obtaining/stations/2123.php (accessed on 1 August 2024)). The MSL was 0.93 m in October 2016, 0.59 m in July 2018, and 0.67 m in August 2023.

The areas of the two prevalent land cover conversions from 2016 to 2023, foredune/strand to scrub/hammock (5.6% of the total Launch AOI) and marsh to mangrove (3.9%), are also indicated in Figure 7. The land cover conversions from marsh to mangrove occurred along the lagoon shores and the conversions from foredune/strand to shrubs/hammock are prominent near SLC-41 and SLC-40 (Figure 7).

3.2. Impacts of Individual Launch on Vegetation

The NDVI changes immediately before and after Falcon Heavy launches at LC-39A (Figure 8Ai,Bi) are compared to the NDVI changes at LC-39B (Figure 8Aii,Bii), a nearby complex where there was no launch during that time frame (Figure 8).

The northern portion of the launchpads (the area indicated with the open red oval in Figure 8) displays reduced NDVI values that were associated with the exhaust plume (Figure 8Ai,Bi). All other areas of NDVI changes greater than 0.1 (such as in Figure 8Bii,Biv) were either due to lawn mowing or growing of the turfgrass (*Personal communication: Tammy Ford and Jeffrey Collins at KSC* [41]). By one month after the launches, the vegetation impacted by the rocket launches as well as the mowed areas recovered, as indicated by the positive NDVI difference values (Figure 8Aiii,Aiv,Biii,Biv).

3.3. Dune Elevation Changes and Beach Erosion

Figure 9 depicts the general elevation trends at the launch and control sites from 2007 to 2018. Prior to 2010, both sites appeared to experience elevation loss. The timing of Tropical Storm Fay in 2008 (15–29 August 2008) is indicated in the plot. From 2010 to 2016, the elevations at the control site were relatively stable while the launch site showed some elevation increases. The elevations at both sites appeared to remain relatively stable through Hurricanes Matthew (28 September–9 October 2016) and Irma (30 August–13 September 2017). A divergence begins to appear in late 2017, with the control site increasing in elevation and that of the launch sites decreasing.

Figure 7. The areas of 2016–2023 land cover (LC) changes from coastal marsh to mangroves (**top left**) and from foredune/strand to coastal scrub/hammock (**top right**). The areas of the LC change from coastal marshes to mangroves at the vicinities of the launchpads are denoted with pink (**bottom left**); and the areas of the LC change from foredune/strand to scrub/hammock are denoted with red (**bottom right**). The maps were created using ArcGIS software and ArcGIS Online basemap by ESRI (Copyright © Esri. All rights reserved).

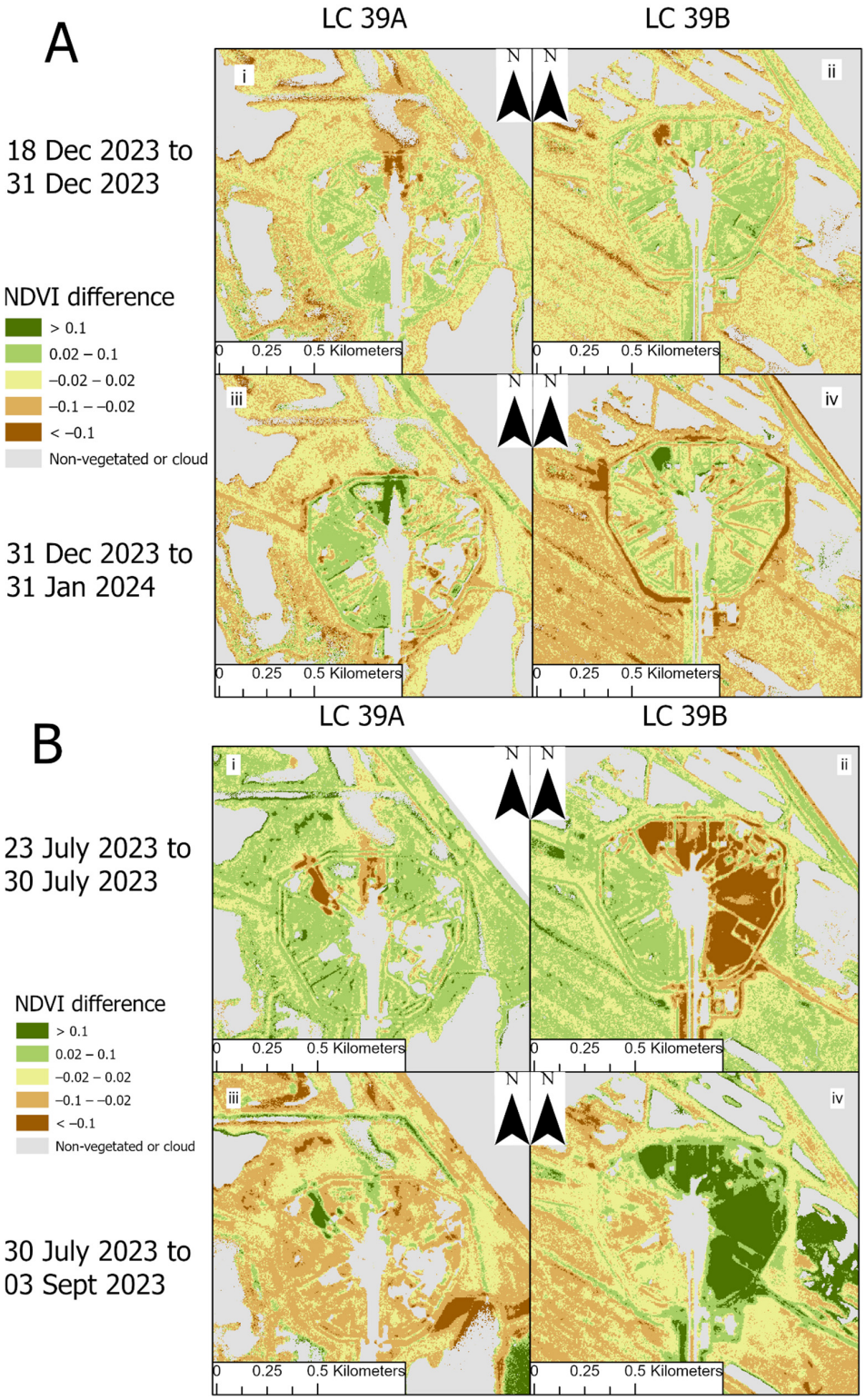

Figure 8. (**A**) Changes in NDVI values on and surrounding Launch Complex (LC)-39A and the nearby LC-39B before, two days after, and about one month after the 28 July 2023 Falcon Heavy rocket launch from LC-39A. (**B**) Changes in NDVI values on and surrounding LC-39A and the nearby LC-39B before, two days after, and about one month after the 28 December 2023 Falcon Heavy rocket launch from LC-39A. The open red oval indicates damage associated with the rocket launches. There was no rocket launch from LC-39B (**Aii**,**Aiv**,**Bii**,**Biv**). (**i**,**ii**) NDVI difference before and two days after rocket launches from LC-39A. (**iii**,**iv**) NDVI changes one month after the rocket launches.

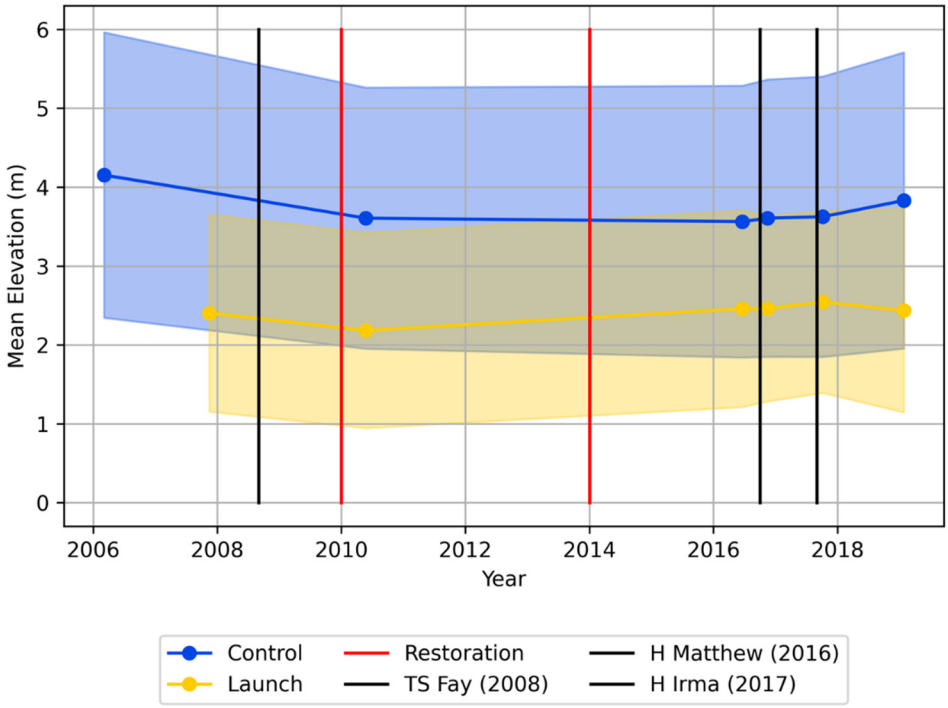

Figure 9. Mean dune elevation for control (Canaveral National Seashore-CANA) and launch sites over time. Shaded area represents one standard deviation. Timings of Tropical Storm Fay, Hurricane Matthew, and Hurricane Irma are indicated.

Dune elevation profile data along the transects at the CANA control site, LC-39A/B, LC-39A with the KSC's dune restoration, and SLC-40/41 are presented in Figure 10 and Table 4. The elevation changes during the 10-year time period (2006/2007 and 2016/2017) were significant for the dunes near LC-39A/B (Figure 10B,C), while the changes at the CANA control site and SLC-40/41 were not significant (Table 4; Figure 10). Notably, the dune elevation between LC-39A and LC-39B was reduced significantly in 2017 (Figure 10B), as the elevation was higher in 2017 compared to that in 2007 at the dunes near LC-39A (Figure 10C), reflecting the effect of the 2013/2014 dune restoration by the KSC.

The dune elevation near LC-39A is 2.4 m lower than that of the control site and 1.1 m lower than the dune elevation near SCL-40/41 (Table 4; Figures 9 and 10). There are also visible areas of erosion of a nearly 50 m beach retreat near LC-39A from 2010 and 2023 (Figure 11).

Figure 12, a kernel density estimation (KDE) plot, denotes the elevation (in meters relative to NAVD88) seen in the early season 2016 LiDAR data for different land cover classes, as identified by the SVM 2016 classification. As with any KDE plot, the peaks in the distribution lines indicate the highest densities of points. The coastal marsh and mangrove classes occupy similar elevation levels and ranges, with mangroves having a slightly higher mean elevation. The scrub hammock and foredune strand also have similar means but their point elevation concentrations are spread out over a much wider range compared to those of coastal marsh and mangrove. The scrub hammock distribution is also bimodal, with two distinct regions of high elevation density.

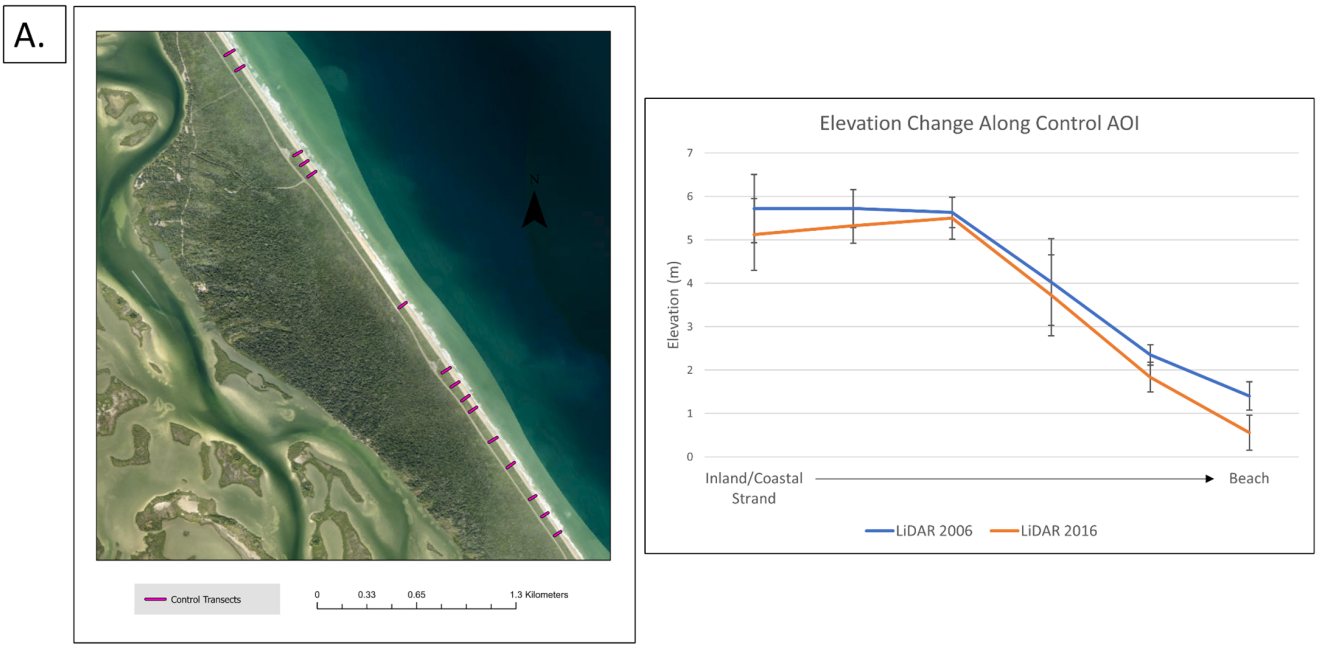

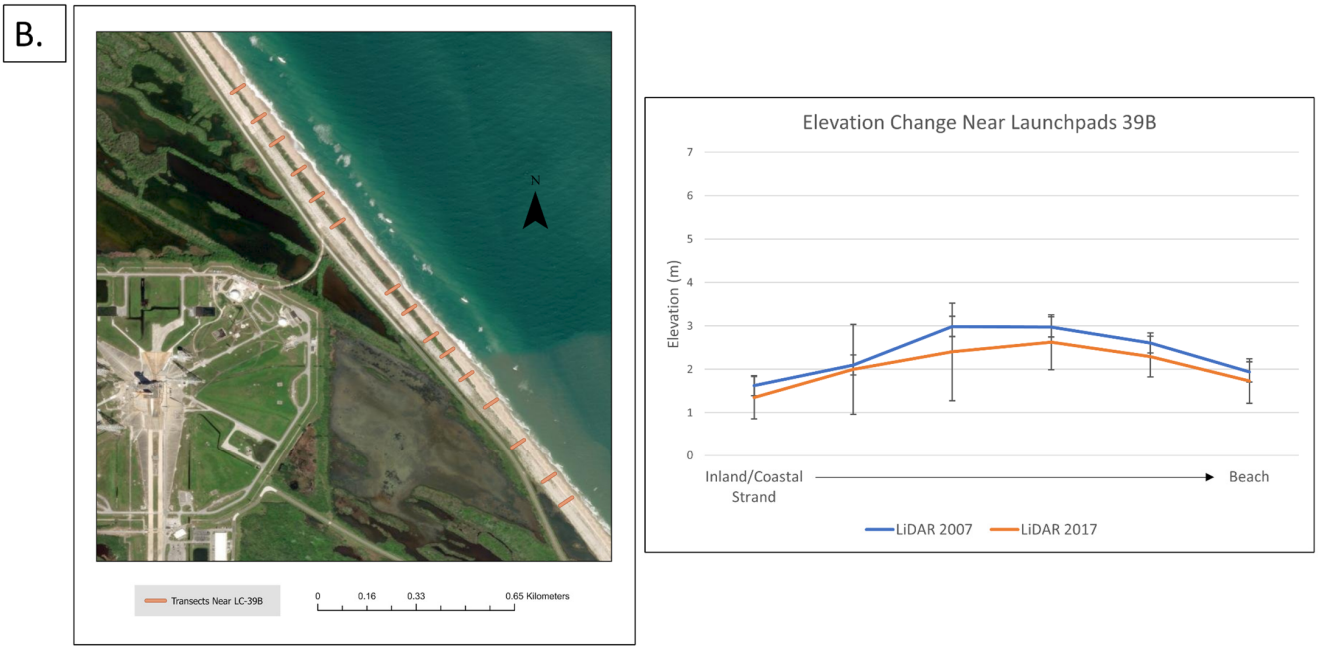

Figure 10. *Cont.*

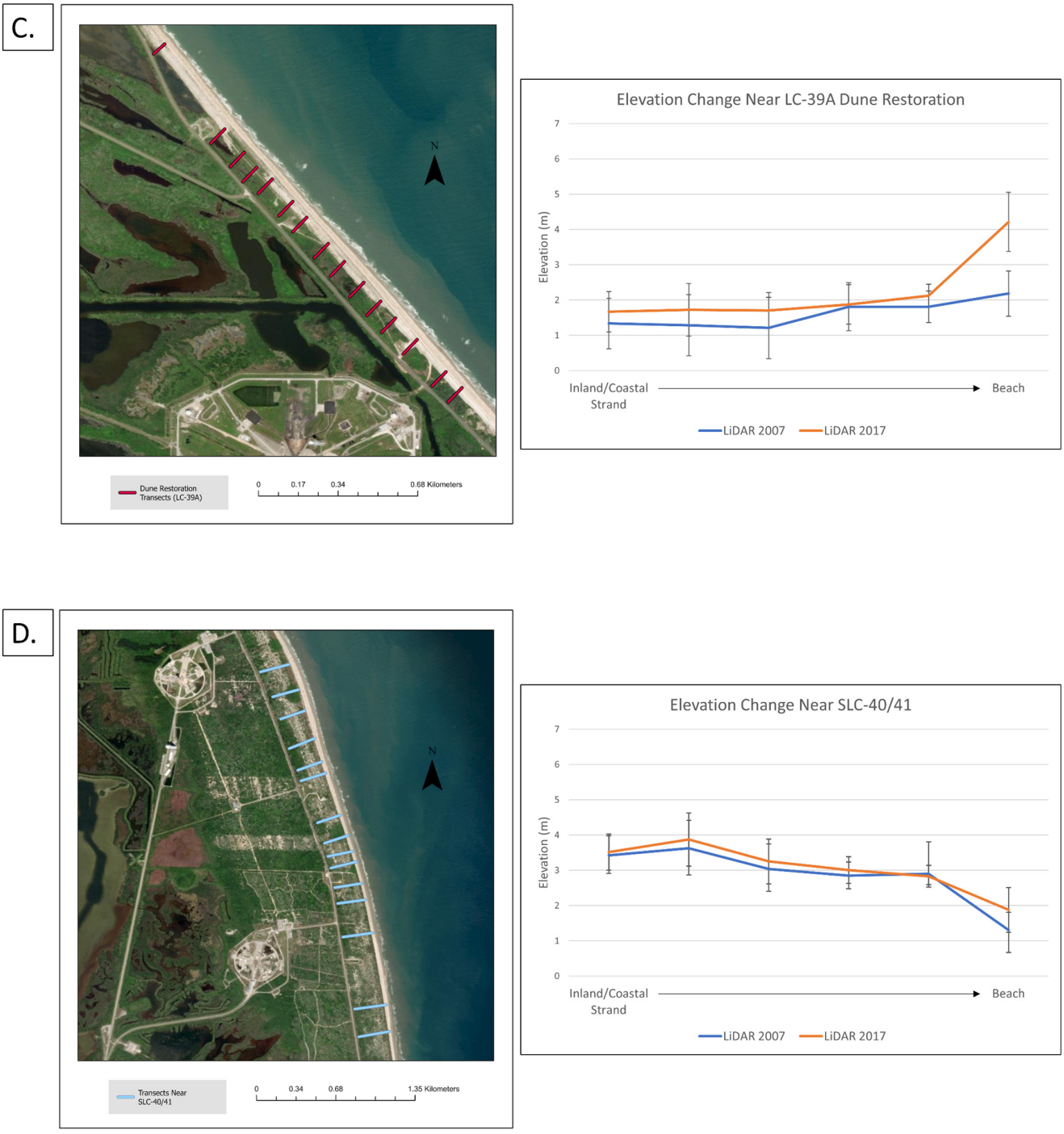

Figure 10. (**A**) dune elevation changes at the control site between 2006 and 2016 (mean transect length is ~50 m). (**B**) dune elevation changes in between Launch Complexes 39A and 39B between 2007 and 2017 (mean transect length is ~45 m). (**C**) dune elevation changes at Launch Complex 39A between 2007 and 2017 (mean transect length is ~45 m). (**D**) dune elevation changes at Space Launch Complex 41 and 40 between 2006 and 2016 (mean transect length is ~200 m). Locations of the 15 transects, perpendicular to the shorelines, used to generate dune elevation profiles (four images on the left). The dune elevation profiles (mean values of the 15 transects at each location) are indicated using blue (2006 for control site and 2007 for launch site) or red lines (2016 for control site and 2017 for launch site). Error bars indicate standard deviation. The extent of the Kennedy Space Center's 2013–2014 dune restoration is indicated with a long red line parallel to the shoreline in C.

Table 4. Comparison between the dune elevations (meters) in 2006 and 2016 at the Canaveral National Seashore (CANA) control site and in 2007 and 2017 at the launch sites. The asterisk (*) denote statistical significance.

	Elevation (2006/2007)	Elevation (2016/2017)	p (T $\leq$ t) Two-Tail
CANA, Control (2006–2016)	4.143 ± 0.523	3.680 ± 0.567	0.107
LC-39A and -39B (2007–2017)	2.373 ± 0.595	2.067 ± 0.710	**0.016** *
LC-39A Dune Restoration Area (2007–2017)	1.744 ± 0.677	2.219 ± 1.094	**<0.001** *
SLC 40 and SLC 41(2007–2017)	2.858 ± 0.642	3.060 ± 0.537	0.145

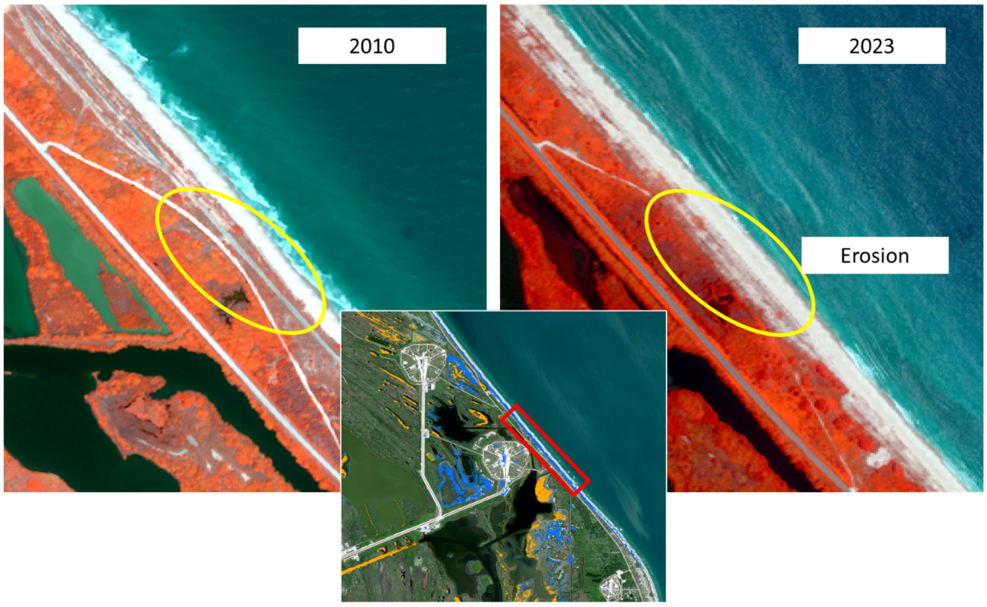

Figure 11. Color infrared images of beach near the Kennedy Space Center's Launch Complex 39A as indicated by the open red rectangle. Beach erosion and dune vegetation loss (a 40–50 m beach retreat between 2010 and 2023) is observed, as indicated by the open yellow oval along the shoreline near LC-39A. WorldView imagery: copyright 2020 DigitalGlobe NextViewLicense.

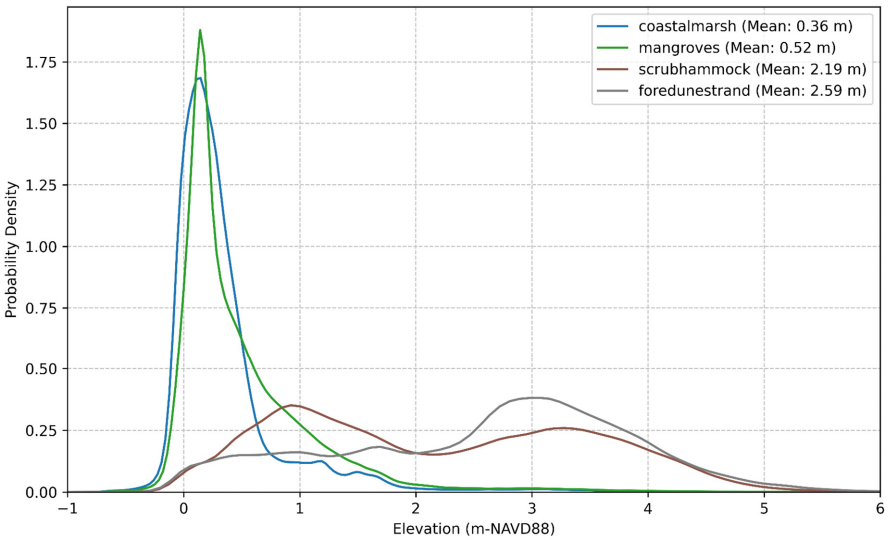

Figure 12. Kernel density estimation plot of elevations across the natural land cover classes from the 2016 SVM classification. The elevations were derived from the 2016 LiDAR data described in Table 3.

3.4. Water Level, Temperature, Prescribed Burns

The water level data of all tide variables display significant increases from 2010 to 2023 (Table 5). The MSL increased over 19 cm and the MLLW increased over 20 cm within the 13-year period. The MLLW trend over the time period (January 2010 through December 2013) was significantly greater than 0 ($p < 0.001$), indicating increases in the local MLLW (Table 5).

Table 5. Annual means and standard deviations of monthly tide data in meters of 2010 and 2023 for the Trident Pier, Port Canaveral, Florida station (ID 8721604). *p*-values obtained from a one-way ANOVA comparing value changes in each of the tide parameters (in meters) between 2010 and 2023. MHHW, MHW, MSL, MTL, and MLLW stand for mean higher high water, mean high water, mean sea level, mean tide level, and mean lower low water, respectively.

		Water Level Change (2010 vs. 2023)							
		Highest	**MHHW**	**MHW**	**MSL**	**MTL**	**MLW**	**MLLW**	**Lowest**
2010	Mean	1.521	1.206	1.094	0.572	0.571	0.049	−0.006	−0.235
	St. Dev.	0.097	0.080	0.090	0.090	0.090	0.092	0.096	0.105
2023	Mean	1.704	1.384	1.265	0.764	0.763	0.261	0.203	−0.045
	St. Dev.	0.147	0.112	0.116	0.118	0.117	0.119	0.124	0.136
Δ mean		0.184	0.178	0.171	0.192	0.191	0.212	0.209	0.190
p-value		0.002	<0.001	0.001	<0.001	<0.001	<0.001	<0.001	0.001

The rate of sea-level rise was calculated from the MSL data and used to display how daily mean water levels might look now and in the future near Launch Complex 39A (Figure 13). Currently, lagoon water already comes close to the launchpad at MSL when only land elevation and tide levels are considered (left map in Figure 13). If sea levels keep rising as expected (at the rate seen in Table 5), by 2084, the water will regularly reach the height of the road surrounding the launchpad at MSL, assuming no other factors affecting the elevation of the area.

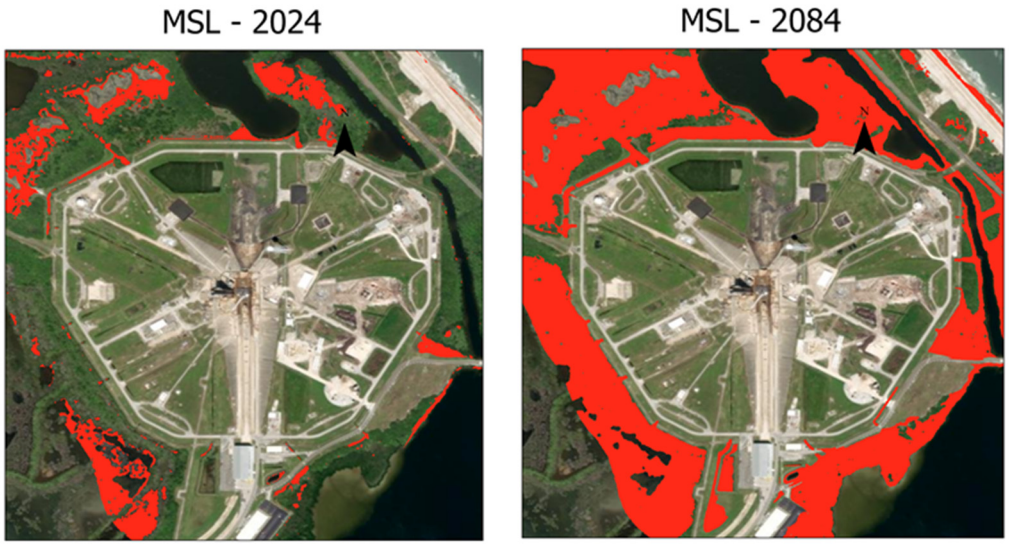

Figure 13. Projected sea-level rise scenarios surrounding LC-39A, based on current mean sea level (MSL, m) from August 2023 to July 2024. The images show MSL water level (red) in 2024 (**left**) and projected in 2084 (**right**) within the land surrounding LC-39A.

MHHW projections from the NOAA Sea Level Rise Viewer show similar patterns: the levels exceed one meter above the baseline year 2000 in two (intermediate high and high) of

the four scenarios for 2080 and three of the four scenarios (intermediate, intermediate high, and high) for 2100 (Figure 14). Much of the area surrounding LC-39A would be submerged at MHHW with a one meter rise (Figure 15). The exception is the area immediately outside the southwest quadrant of LC-39A, which is not directly hydrologically connected to the ocean but which has already displayed visual indications of a rising water level, in agreement with the 2024 map in Figure 13.

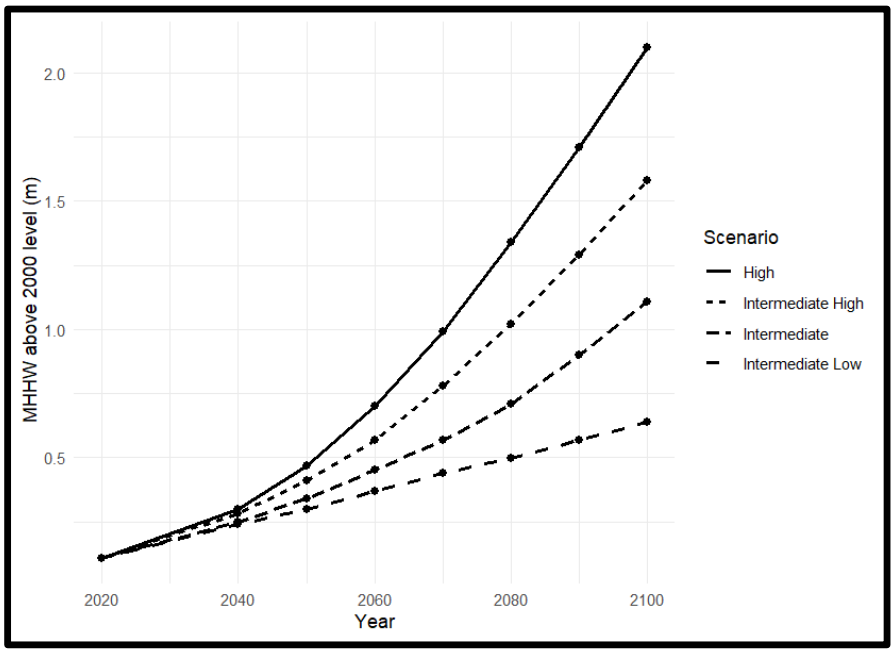

Figure 14. Projected MHHW levels at Trident Pier relative to the year 2000 from the NOAA Sea Level Rise Viewer.

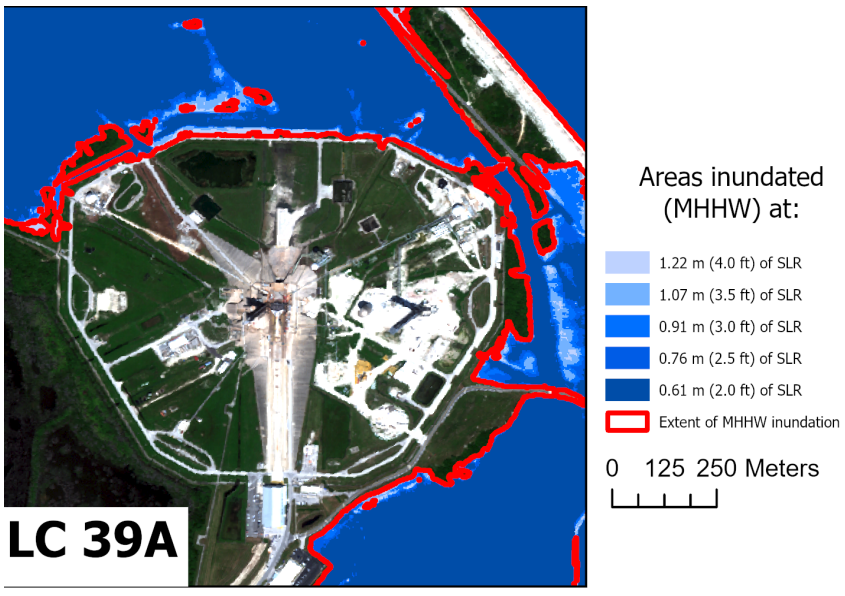

Figure 15. Areas surrounding LC-39A that are hydrologically connected to the ocean and would be inundated at various levels of MHHW that are possible by 2080.

The daily minimum temperature trend is generally projected to reach at or below 0 °C less than three–four days per year (Figure 16). There were 11 days with freezing conditions in 2005 and 14 days in 2010 (Figure 16). There were 11 consecutive days out of the total of 14 days that reached below 0 °C in 2010 (Figure 16).

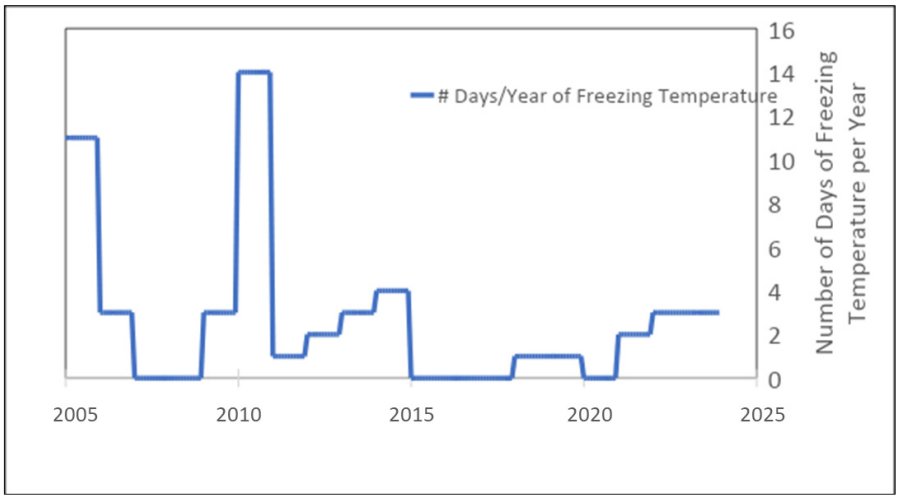

Figure 16. Number of days reaching at or below the freezing temperature (0 °C) per year between January 2005 and December 2023. Air temperature data were collected from the Global Historical Climatology Network daily (GHCNd) station near the Kennedy Space Center (Merritt Island, FL, USA).

Figure 17 displays the areas of burns from prescribed fires (left) along with the land cover change (from 2016 to 2023) hot spot map (right). The areas from the west to the southwest of LC-39B were burned in 2012 and again in 2017. The most recent prescribed fires near SLC-41 and -41 were in 2011. The land cover change hot spot areas (indicated with red-orange hues in the right panel of Figure 17) encompass the locations of LC-39A, SLC-41, and SLC-40 (Figures 3 and 17 left), the location of 2017 burns to the west of LC-39B which resulted in the loss of mangroves (Figures 7 and 17), and the lack of recent burns (the last burns occurred in 2011) near SLC-40/41 which resulted in strand-to-hammock conversion (Figures 7 and 17). The physical location of LC-39B, which was not used for launches during the study period except for one launch in November 2022, was not included in the hot spots while all other launchpads were within the hot spots (Figure 17). Cold spots indicate areas that are stable and exhibit a significant lack of land cover change; these are largely water bodies whose extent has not been substantially affected between 2016 and 2023.

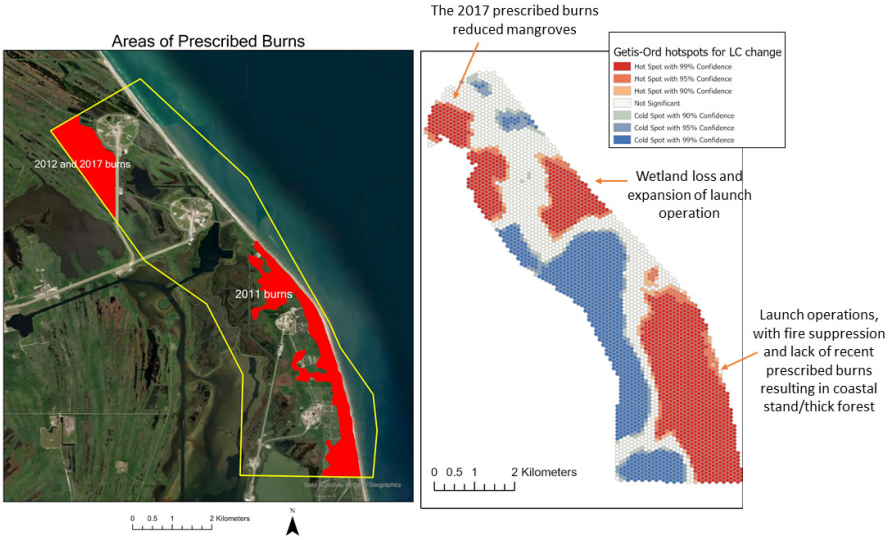

Figure 17. Left: areas of burns from prescribed fires in 2011 (low right red polygon) and 2012/2017 (upper left red polygon). The data were obtained from the Monitoring Trends in Burn Severity (MTBS) website (mtbs.gov). **Right**: land cover change (from 2016 to 2023) hot spot map is presented to compare the locations of burns.

4. Discussion & Conclusions

The landscape of Cape Canaveral Barrier Island changes in response to regional climate variability and shifts in land use, which are driven by interactions among climatic, environmental, and anthropogenic factors, as with other ecosystems [40]. The area's natural habitats range from sandy beaches and dunes along the Atlantic Ocean; to upland habitats such as coastal strands, scrubs, and maritime hammocks; to estuarine wetlands like mangroves and saltmarshes (Figure 3). These ecosystems are vital for biodiversity, supporting species including federally listed manatees, beach mice, sea turtles, and scrub jays, and providing ecosystem services like sediment stabilization, coastal erosion control, and carbon sequestration [29,42]. This study documented and demonstrates the increasing challenges to maintaining the system's balance exerted by multiple, interconnected factors, including fire management (prescribed fires or fire suppression; Figure 17), sea-level rise (Table 5, Figures 13–15), wetland community changes with a deficiency of winter freezes (Figures 5, 7 and 16), storm-driven dune loss and beach erosion (Figures 9–11; Table 4), mosquito control diking and wetland loss (Figure 6), and the expanding footprint of space launch operations (Figures 2 and 8).

The spectral classification process in this study encountered challenges in accurately distinguishing between scrub/hammock and mangrove habitats, as well as between scrub/hammock and strand habitats, at both the control (Figure 2) and launch sites (Figure 3), even with the use of high-resolution (2 m) eight-band WorldView imagery. This confusion arises due to the spectral similarities between hardwood hammock trees and mangroves [43], as well as the shared plant species and gradual community gradients across coastal strands, scrubs, and maritime hammock habitats [30]. Despite these challenges, the classification differentiates upland vegetation with a sandy background (classified as foredune/strand with higher reflectance in the visible wavelengths), hammock with a dense canopy (the largest reflectance difference between the visible and near-infrared regions), wetland areas characterized by lower infrared reflectance, and herbaceous wetlands from wooded wetlands (Figure 4).

The significant land cover changes between 2016 and 2023 include the expansion of mangroves in the lagoon-side wetland areas and the conversion of open shrubby strands and scrubs to taller, denser scrubs and hammock trees (Figures 5 and 7). The transition from saltmarsh to mangrove has been well-documented in Florida [17] and other regions [38], driven by the reduced frequency and duration of hard freezes, which facilitates the northward migration of mangroves in the northern hemisphere. Freezing conditions in this area rarely persist for more than two consecutive days per year, except during strong La Niña winters (e.g., the 2010/2011 La Niña) [44]. For instance, during the winter of 2010, 11 consecutive days had sub-0 °C temperatures in the study area (Figure 16). In 6 of the past 18 years, there were no freezing days at all, and since 2016, low temperatures have not been severe or prolonged enough to exceed the tolerance levels of mangroves (Figure 16) [37].

The widespread conversion from foredune/strand to scrub/hammock near SLC-40/-41 (Figures 5 and 7) appears to be linked to the absence of recent fires in the area (Figure 17). The last prescribed burn was conducted in 2011. Fire is an important mechanism in maintaining scrub in this region [39]. Since 1992, mechanical treatments and prescribed burns have been used to help maintain scrub vegetation in order to enhance the habitat for the Florida scrub-jay. Schmalzer and Adrian (2001) [39] observed that scrub vegetation in long-unburned areas grows more quickly than in regularly burned areas, which was demonstrated in this study (Figures 5, 7 and 17). Shrubby vegetation in well-drained sandy soils provides essential habitats for several species, including several endemic and listed Florida scrub-dependent species. In contrast, in the area west of LC-39B, where relatively recent burns have occurred (Figures 5, 7 and 17), mangrove growth appears to have been suppressed. Fire plays a key role in preventing the establishment of mangroves, which typically thrive in fire-suppressed or wetter environments.

Wetland loss near LC-39A (Figure 6) occurred within the impounded area [11]. Mosquito control impoundments in this region were constructed in the 1950s and 1960s by

dredging around salt marshes to create earthen dikes, with water control structures like culverts and pumps allowing seasonal water flow. This rotational impoundment management (RIM) system, where culverts are closed in the wet season and opened in the fall, has been an effective means of mosquito control. However, these impoundments and the RIM alter the natural hydrology of saltmarshes, leading to reduced tidal flow and altered water quality, which can degrade salt marshes over time [45].

The dune elevation at the Cape Canaveral launch site is considerably lower than that at the control site in CANA (Figures 9 and 10; Table 4). Due to its proximity to the beach and dunes, LC-39A/B face significant threats from dune erosion (Figure 10) and beach retreat (Figure 11). As an adaptive management strategy, NASA implemented dune restoration in 2010 and again in 2013/2014 to address erosion hot spots near LC-39A (Figure 10C) [16]. The impact of these efforts is evident, with the overall dune elevation at the launch site increasing between 2010 and 2018 (Figure 9), as well as in the dune profile comparison between 2007 and 2017 (Figure 10C). Visible erosion persisted near LC-39A between 2010 and 2023, making it a designated erosion hot spot where sandy dune construction was implemented in 2013/2014 [16].

Tide levels have risen significantly in this area (Table 5; Figure 11), with increases in the mean lower low water (MLLW) indicating that more upland habitats will be affected by rising water tables, salinity changes, and root zone saturation [34,35]. Although this study did not find noticeable expansion in wetlands compared to the upland areas, previous studies predicted much of the coastal uplands to be converted to mangrove wetlands [3,11]. It is understood that each natural land cover type generally thrives in a specific topography (Figure 12). For coastal land cover types, their optimal topography is mostly determined by their vertical position in the tide range and the resulting hydroperiod, or wetting and drying cycle. The mean elevation values for the natural land cover types at the launch site broadly agree with those presented in Foster et al. (2017), although the classification schema is different [3] (Figure 11). The future landscape dynamics driven by launch operation effects, climate change, topographic changes from storm erosion, sea-level rise, and the natural and prescribed burn regime will be interesting and essential knowledge for a variety of coastal stakeholders.

Launch Complex 39A faces imminent challenges, including wetland loss on the lagoon side (Figure 6), dune and beach erosion on the ocean side (Figures 10, 11 and 13–15), and increases in tide levels (Table 4; Figures 11 and 13–15). And the additional compounding factor is the increasing volume and scale of rocket launches and operations using this complex.

The space industry is essential for space exploration and the local and national economy [46]. However, the increasing frequency and intensity of rocket launches and the proposed and tentatively upcoming Starship-Super Heavy launches present additional challenges. Presently (2024), the US Department of the Air Force (DAF) is preparing an environmental impact statement (EIS; https://spaceforcestarshipeis.com/ (accessed on 1 August 2024)) to assess the potential environmental impacts of SpaceX's proposals to construct and operate facilities for Starship and Super Heavy launch vehicles at Cape Canaveral, particularly at LC-39A.

The Falcon 9, Falcon Heavy, and Starship rockets developed by SpaceX are designed to serve different purposes of space exploration and satellite deployment (https://www.spacex.com/ (accessed on 1 August 2024)). The Falcon 9 is 70 m tall and can carry payloads up to 22,800 kg to low Earth orbit (LEO) and 8300 kg to geostationary transfer orbit (GTO). Falcon Heavy, also 70 m tall, comprises three Falcon 9 cores working in tandem and able to deliver 63,800 kg to LEO and 26,700 kg to GTO. Starship, with a height of 120 m and a diameter of 9 m, is designed to carry over 100,000 kg to LEO and significant payloads beyond.

While the exhaust from engines burning LOx propellant, used in Falcon rockets, primarily consists of water vapor, the exhaust still produces nitrous oxide as the hot exhaust gases heat the air [20,47]. Kerosene, commonly used in the first stage of rocket launches for

its high density and handling ease compared to LOx, raises fewer environmental concerns than hypergolic propellants (a.k.a. devil's venom) and solid propellants, but still emits CO_2 and soot particles, significant contributors to global climate change. Starship uses methane as a fuel as opposed to kerosene.

According to the results of our study, the impacts of Falcon rocket launches on nearby vegetation are less (Figure 8) than those documented for the cases using SRM fuels [11,21–24]. The ground cloud, formed from the interaction of exhaust from solid rocket boosters with deluge water, led to vegetation changes from the repeated near-field deposition of aluminum oxide and hydrochloric acid. The near-field deposition was commonly seen within 1.5 km; and far-field deposition effects, which expanded to the extent of the barrier island in some cases, from the SRM propellants included acid deposition and spotting on plant leaves.

Most of the vegetation impacts seen in this study that are associated with the Falcon Heavy launches were within the vicinity of the launchpad, and the vegetation recovered within a one-month period after the launch events (Figure 8). The northern portion of the launchpads (area indicated with the open red circles in Figure 8) displays reduced NDVI values that were associated with the rockets' exhaust plumes (Figure 8Ai,Bi). Falcon rocket exhaust is channeled through nozzles to direct the high-pressure gases from combustion; during maneuvers, the exhaust plume can shift to one side temporarily to help steer the rocket (https://www.youtube.com/watch?v=976LHTpnZkY&t=15s (accessed on 1 August 2024)). The wind direction and speed at the time of the launch do not dictate the direction and expanse of the plume because of the directed release of the exhaust plume and also because most successful launches occur when the winds are calm.

The launch sites are located in sensitive coastal areas already facing chronic stressors such as sea-level rise, shifting weather patterns, and fire suppression, alongside pulse disturbances from storms, hurricanes, and human activities like construction and fire/habitat management. These compounded pressures drive changes in coastal ecosystems at a pace faster than natural recovery processes [48], threatening the resilience of launchpads, other infrastructure, and launch operations. As the space industry grows, the cumulative environmental impacts of an increased launch frequency and volume need to be carefully monitored and managed. Federal and local stakeholders are responsible for balancing operational demands with environmental stewardship to ensure the sustainable coexistence of space exploration and the conservation of this barrier island, which is home to numerous endemic and listed species.

The interplay between vegetation changes and dune erosion on barrier islands is fundamental to the ecosystem's resilience, as healthy plant communities stabilize dunes, while erosion can lead to vegetation loss, creating a detrimental feedback loop that exacerbates both habitat degradation and infrastructure vulnerability [49]. The systematic integration of sustainable management practices, such as dune restoration and restoring critical habitats (e.g., coastal scrubs), would be essential to mitigate these interactions, ensuring both the resilience of the ecosystem and the protection of infrastructure against future climate challenges.

In conclusion, this study found that: (1) there have been changes in the coastal vegetation community, with notable conversions from saltmarshes to mangroves in the wetland area and from coastal strand and open scrubs to densely vegetated hardwood forests in upland areas; (2) the impacts of rocket launches using the liquid propellant on nearby vegetation are detectable using high-resolution satellite imagery, but the damage scale is smaller than that of the solid rocket engine vehicles; and (3) there is a forthcoming threat of inundation to areas of LC-39A/B with increasing tide levels, dune and beach erosion, and loss of the surrounding wetlands.

Author Contributions: Conceptualization, H.J.C., M.J.M., S.C.M., H.V.H., C.D.C.J. and C.M.J.; methodology, H.J.C., D.B., K.M.S.A., M.J.M., S.C.M. and H.V.H.; validation, H.J.C., K.M.S.A. and D.B.; formal analysis, H.J.C., D.B., K.M.S.A. and H.V.H.; investigation, H.J.C., D.B. and K.M.S.A.; resources, H.J.C., D.B. and M.J.M.; data curation, M.J.M., D.B., H.J.C. and S.C.M.; writing—original

draft preparation, H.J.C., K.M.S.A., D.B. and S.C.M.; writing—review and editing, M.J.M., K.M.S.A., H.V.H., H.J.C., D.B. and Y.Z.; visualization, H.J.C., D.B., K.M.S.A., M.J.M. and S.C.M.; supervision, H.J.C. and C.D.C.J.; project administration, H.J.C., C.D.C.J. and C.M.J.; funding acquisition, H.J.C. All authors have read and agreed to the published version of the manuscript.

Funding: This research was supported in part by an appointment to the Department of Defense (DOD) Research Participation Program administered by the Oak Ridge Institute for Science and Education (ORISE) through an interagency agreement between the U.S. Department of Energy (DOE) and the DOD. ORISE is managed by ORAU under DOE contract number DE-SC0014664. All opinions expressed in this paper are the author's and do not necessarily reflect the policies and views of DOD, DOE, or ORAU/ORISE. This research was made possible by the NASA MUREP DEAP project funded by the National Aeronautics and Space Administration 80 NSSC 23 M 0053), the National Oceanic and Atmospheric Administration (NOAA), Office of Education, Educational Partnership Program with Minority-Serving Institutions award #NA21SEC4810004 (NOAA Center for Coastal and Marine Ecosystems—II), and the Department of Education's Title III funds to Bethune-Cookman University. The contents of this publication are solely the responsibility of the award recipient and do not necessarily represent the official views of the U.S. Department of Defense, Department of Commerce, NOAA, or NASA. Any opinions, findings, conclusions, or recommendations expressed in this presentation are those of the authors and do not necessarily reflect the view of the funding agencies.

Data Availability Statement: All publicly available data presented in this study are cited with the URLs in the text. The satellite data and products presented in this study are available on request from the corresponding author due to the conditions for the limited data access permitted by the National Geospatial-Intelligence Agency.

Acknowledgments: The authors extend their gratitude to Tammy Foster and Jeffrey S. Collins at Kennedy Space Center for generously sharing their resources and expertise.

Conflicts of Interest: The authors declare no conflicts of interest.

References

1. Johnson, J.M.; Moore, L.J.; Ells, K.; Murray, A.B.; Adams, P.N.; MacKenzie III, R.A.; Jaeger, J.M. Recent shifts in coastline change and shoreline stabilization linked to storm climate change. *Earth Surf. Process. Land.* **2015**, *40*, 569–585. [CrossRef]
2. Vitale, N.; Brush, J.; Powell, A. Loss of Coastal Islands Along Florida's Big Bend Region: Implications for Breeding American Oystercatchers. *Estuar. Coast.* **2021**, *44*, 1173–1182. [CrossRef]
3. Foster, T.E.; Stolen, E.D.; Hall, C.R.; Schaub, R.; Duncan, B.W.; Hunt, D.K.; Drese, J.H. Modeling vegetation community responses to sea-level rise on barrier island systems: A case study on the Cape Canaveral Barrier Island complex, Florida, USA. *PLoS ONE* **2017**, *12*, e0182605. [CrossRef] [PubMed]
4. Mucova, S.A.R.; Azeiteiro, U.M.; Filho, W.L.; Lopes, C.L.; Dias, J.M.; Pereira, M.J. Approaching sea-level rise (SLR) change: Strengthening local responses to sea-level rise and coping with climate change in northern Mozambique. *J. Mar. Sci. Eng.* **2021**, *9*, 205. [CrossRef]
5. Defeo, O.; McLachlan, A.; Schoeman, D.S.; Schlacher, T.A.; Dugan, J.; Jones, A.; Lastra, M.; Scapini, F. Threats to sandy beach ecosystems: A review. *Estuar. Coast. Shelf S.* **2009**, *81*, 1–12. [CrossRef]
6. Prosser, D.J.; Jordan, T.E.; Nagel, J.L.; Seitz, R.D.; Weller, D.E.; Whigham, D.F. Impacts of Coastal Land Use and Shoreline Armoring on Estuarine Ecosystems: An Introduction to a Special Issue. *Estuar. Coast.* **2018**, *41* (Suppl. S1), 2–18. [CrossRef]
7. Singh, V.P.; Mishra, A.K.; Chowdhary, H.; Khedun, C.P. Climate Change and Its Impact on Water Resources. In *Modern Water Resources Engineering*; Humana Press: Totowa, NJ, USA, 2014; pp. 525–569. [CrossRef]
8. Griggs, G.; Reguero, B.G. Coastal adaptation to climate change and sea-level rise. *Water* **2021**, *13*, 2151. [CrossRef]
9. Mousavi, M.E.; Irish, J.L.; Frey, A.E.; Olivera, F.; Edge, B.L. Global warming and hurricanes: The potential impact of hurricane intensification and sea level rise on coastal flooding. *Clim. Change* **2011**, *104*, 575–597. [CrossRef]
10. Oppenheimer, M.; Glavovic, B.C.; Hinkel, J.; van de Wal, R.; Magnan, A.K.; Abd-Elgawad, A.; Cai, R.; Cifuentes-Jara, M.; DeConto, R.M.; Ghosh, T.; et al. Sea Level Rise and Implications for Low-Lying Islands, Coasts and Communities. In *IPCC Special Report on the Ocean and Cryosphere in a Changing Climate*; Pörtner, H.-O., Roberts, D.C., Masson-Delmotte, V., Zhai, P., Tignor, M., Poloczanska, E., Mintenbeck, K., Alegría, A., Nicolai, M., Okem, A., et al., Eds.; Cambridge University Press: Cambridge, UK; New York, NY, USA, 2019; pp. 321–445. [CrossRef]
11. Hall, C.R.; Schmalzer, P.A.; Breininger, D.R.; Duncan, B.W.; Drese, J.H.; Scheidt, D.A.; Lowers, R.H.; Reyier, E.A.; Holloway-Adkins, K.G.; Oddy, D.M.; et al. Ecological Impacts of the Space Shuttle Program at John F. Kennedy Space Center, Florida. No. KSC-E-DAA-TN12459, 1 January. 2014. Available online: https://ntrs.nasa.gov/citations/20140012489 (accessed on 30 September 2024).

12. Brockmeyer, R.E., Jr.; Donnelly, M.; Rey, J.R.; Carlson, D.B. Manipulating, managing and rehabilitating mangrove-dominated wetlands along Florida's east coast (USA): Balancing mosquito control and ecological values. *Wetl. Ecol. Manag.* **2022**, *30*, 987–1005. [CrossRef]
13. Schmalzer, P.A.; Foster, T.E.; Adrian, F.W. Responses of Long-Unburned Scrub on the Merritt Island/Cape Canaveral Barrier Island Complex to Cutting and Burning. In Proceedings of the Second International Wildland Fire Ecology and Fire Management Congress and Fifth Symposium on Fire and Forest Meteorology, Orlando, FL, USA, 16–20 November 2003; American Meteorological Society: Boston, MA, USA, 2003; p. 6. Available online: https://ams.confex.com/ams/pdfpapers/65188.pdf (accessed on 1 August 2024).
14. Schmalzer, P.A.; Hinkle, C.R. Effects of Fire on Composition, Biomass, and Nutrients in Oak Scrub Vegetation on John F. Kennedy Space Center, Florida. NASA Technical Memorandum 100305, 1 July. 1987. Available online: https://ntrs.nasa.gov/citations/19880006800 (accessed on 30 September 2024).
15. Hall, C. Hydrologic Baseline Conditions and Projected Trends for Kennedy Space Center and the Cape Canaveral Barrier Island Complex. 2021. Available online: https://ntrs.nasa.gov/citations/20210022830 (accessed on 13 August 2024).
16. Bolt, M.R.; Mercadante, M.A.; Kozusko, T.J.; Weiss, S.K.; Hall, C.R.; Provancha, J.A.; Cancro, N.R.; Foster, T.E.; Stolen, E.D.; Martin, S.A. An adaptive managed retreat approach to address shoreline erosion at the Kennedy Space Center, Florida. *Ecol. Restor.* **2019**, *37*, 171–181. [CrossRef]
17. Radabaugh, K.R.; Powell, C.E.; Moyer, R.P. *Coastal Habitat Integrated Mapping and Monitoring Program Report for the State of Florida*; Florida Fish and Wildlife Conservation Commission; Technical Report No. 21; Fish and Wildlife Research Institute: St. Petersburg, FL, USA, 2017.
18. Reed, D.C.; Schmitt, R.J.; Burd, A.B.; Burkepile, D.E.; Kominoski, J.S.; McGlathery, K.J.; Miller, R.J.; Morris, J.T.; Zinnert, J.C. Responses of Coastal Ecosystems to Climate Change: Insights from Long-Term Ecological Research. *BioScience* **2022**, *72*, 871–888. [CrossRef]
19. Ryan, R.G.; Marais, E.A.; Balhatchet, C.J.; Eastham, S.D. Impact of rocket launch and space debris air pollutant emissions on stratospheric ozone and global climate. *Earth's Futur.* **2022**, *10*, e2021EF002612. [CrossRef] [PubMed]
20. Dallas, J.A.; Raval, S.; Gaitan, J.A.; Saydam, S.; Dempster, A.G. The environmental impact of emissions from space launches: A comprehensive review. *J. Clean. Prod.* **2020**, *255*, 120209. [CrossRef]
21. Schmalzer, P.A.; Hinkle, C.R.; Breininger, D.; Knott, W.M., III; Koller, A.M., Jr. Effects of Space Shuttle Launches STS-1 Through STS-9 on Terrestrial Vegetation of John F. Kennedy Space Center, Florida. NASA Technical Memorandum 83103, 1 September 1985. Available online: https://ntrs.nasa.gov/citations/19870011225 (accessed on 1 August 2024).
22. Schmalzer, P.A.; Hinkle, C.R.; Dreschel, T. Far-Field Deposition from Space Shuttle Launches at John F. Kennedy Space Center, Florida. NASA Technical Memorandum 83104, 1 December 1986. Available online: https://www.researchgate.net/publication/24302733_Far-field_deposition_from_space_shuttle_launches_at_John_F_Kennedy_Space_Center_Florida (accessed on 30 September 2024).
23. Schmalzer, P.; Hall, C.; Hinkle, C.; Duncan, B.; Knott, W., III; Summerfield, B. Environmental Monitoring of Space Shuttle Launches at Kennedy Space Center—The First Ten Years. In Proceedings of the 31st Aerospace Sciences Meeting, Reno, NV, USA, 11–14 January 1993; p. 303. [CrossRef]
24. Schmalzer, P.A.; Boyle, S.R.; Hall, P.; Oddy, D.M.; Hensley, M.A.; Stolen, E.D.; Duncan, B.W. Monitoring Direct Effects of Delta, Atlas, and Titan Launches from Cape Canaveral Air Station. NASA Technical Report 207912, 1 June 1998. Available online: https://ntrs.nasa.gov/api/citations/19980235583/downloads/19980235583.pdf (accessed on 1 August 2024).
25. Foster, T. (Kennedy Space Center, Merritt Island, FL, USA). Personal communication, 2024.
26. Peel, M.C.; Finlayson, B.L.; McMahon, T.A. Updated world map of the Köppen-Geiger climate classification, Hydrol. *Earth Syst. Sci.* **2007**, *11*, 1633–1644. [CrossRef]
27. National Centers for Environmental Information. U.S. Climate Normals: Monthly Climate Normals for Cape Canaveral, Florida. 2024. Available online: https://www.ncei.noaa.gov/access/us-climate-normals/#dataset=normals-monthly&timeframe=15&location=FL&station=US1FLBV0012 (accessed on 1 August 2024).
28. McCarthy, M.J.; Jessen, B.; Barry, M.J.; Figueroa, M.; McIntosh, J.; Murray, T.; Schmid, J.; Muller-Karger, F.E. Mapping hurricane damage: A comparative analysis of satellite monitoring methods. *Int. J. Appl. Earth Obs.* **2020**, *91*, 102134. [CrossRef]
29. Schmalzer, P.A.; Hinkle, C.R. Species Composition and Structure of Oak-Saw Palmetto Scrub Vegetation. *Castanea* **1992**, *57*, 220–251. Available online: https://www.jstor.org/stable/4033733 (accessed on 1 August 2024).
30. Schmalzer, P.A.; Foster, T.E. Flora and Threatened and Endangered Plants of Canaveral National Seashore, Florida. *Castanea* **2016**, *81*, 91–127. [CrossRef]
31. Cho, H.J.; Jarrett, R. *Plants of Atlantic Center for the Arts*; Bethune-Cookman University Press: New Smyrna Beach, FL, USA, 2016; 130p.
32. Spence, D.; Cho, H.J.; Jarrett, R. *Plants of Canaveral National Seashore*; Friends of Canaveral: New Smyrna Beach, FL, USA, 2018; 207p.
33. Jawak, S.D.; Luis, A.J. Improved land cover mapping using high resolution multiangle 8-band WorldView-2 satellite remote sensing data. *J. Appl. Remote Sens.* **2013**, *7*, 073573. [CrossRef]
34. FitzGerald, D.M.; Fenster, M.S.; Argow, B.A.; Buynevich, I.V. Coastal impacts due to sea-level rise. *Annu. Rev. Earth Pl. Sc.* **2008**, *36*, 601–647. [CrossRef]

35. Hopkinson, C.S.; Wolanski, E.; Cahoon, D.R.; Perillo, G.M.; Brinson, M.M. Coastal wetlands: A synthesis. In *Coastal Wetlands*; Elsevier: Amsterdam, The Netherlands, 2019; pp. 1–75. [CrossRef]
36. Guyot-Téphany, J.; Trouillet, B.; Diederichsen, S.; Juell-Skielse, E.; Thomas, J.B.E.; McCann, J.; Rebours, C.; Scherer, M.; Freeman, P.; Gröndahl, F.; et al. Two decades of research on ocean multi-use: Achievements, challenges and the need for transdisciplinarity. *NPJ Ocean Sustain.* **2024**, *3*, 8. [CrossRef]
37. Osland, M.J.; Day, R.H.; Michot, T.C. Frequency of Extreme Freeze Events Controls the Distribution and Structure of Black Mangroves (*Avicennia germinans*) Near Their Northern Range Limit in Coastal Louisiana. *Divers. Distrib.* **2020**, *26*, 1366–1382. [CrossRef]
38. Wang, Y.S.; Gu, J.D. Ecological Responses, Adaptation and Mechanisms of Mangrove Wetland Ecosystem to Global Climate Change and Anthropogenic Activities. *Int. Biodeterior. Biodegrad.* **2021**, *162*, 105248. [CrossRef]
39. Schmalzer, P.A.; Adrian, F.W. Scrub Restoration on Kennedy Space Center/Merritt Island National Wildlife Refuge, 1992–2000. In Proceedings of the Florida Scrub Symposium 2001, Orlando, FL, USA, 5–7 June 2001; pp. 17–20.
40. Cao, Q.; Liu, Y.; Georgescu, M.; Wu, J. Impacts of landscape changes on local and regional climate: A systematic review. *Landscape Ecol.* **2020**, *35*, 1269–1290. [CrossRef]
41. Ford, T.; Collins, J. (Kennedy Space Center, Merritt Island, FL, USA). Personal communication, 2024.
42. Oddy, D.M.; Stolen, E.D.; Schmalzer, P.A.; Hensley, M.A.; Hall, P.; Larson, V.L.; Turek, S.R. Environmental conditions and threatened and endangered species populations near the Titan, Atlas, and Delta launch complexes, Cape Canaveral Air Station. No. NASA/TM-1999-208553, 1 June. 1999. Available online: https://ntrs.nasa.gov/citations/20090007547 (accessed on 30 September 2024).
43. Wendelberger, K.S.; Gann, D.; Richards, J.H. Using Bi-Seasonal Worldview-2 Multi-Spectral Data and Supervised Random Forest Classification to Map Coastal Plant Communities in Everglades National Park. *Sensors* **2018**, *18*, 829. [CrossRef] [PubMed]
44. Boening, C.; Willis, J.K.; Landerer, F.W.; Nerem, R.S.; Fasullo, J. The 2011 La Niña: So strong, the oceans fell. *Geophys. Res. Lett.* **2012**, *39*, L19602. [CrossRef]
45. Rey, J.R.; Walton, W.E.; Wolfe, R.J.; Connelly, R.; O'Connell, S.M.; Berg, J.; Sakolsky-Hoopes, G.E.; Laderman, A.D. North American Wetlands and Mosquito Control. *Int. J. Env. Res. Pub. Health* **2012**, *9*, 4537–4605. [CrossRef]
46. George, K.W. The economic impacts of the commercial space industry. *Space Policy* **2019**, *47*, 181–186. [CrossRef]
47. Kokkinakis, I.W.; Drikakis, D. Atmospheric pollution from rockets. *Phys. Fluids* **2022**, *34*, 056107. [CrossRef]
48. Hawkins, S.J.; Allcock, A.L.; Bates, A.E.; Evans, A.J.; Firth, L.B.; McQuaid, C.D.; Todd, P.A. Human pressures and the emergence of novel marine ecosystems. *Oceanogr. Mar. Biol.* **2020**, *58*, 441–494.
49. San Antonio, K.M.; Burow, D.; Cho, H.J.; McCarthy, M.J.; Medeiros, S.C.; Zhou, Y.; Herrero, H.V. Data-Driven Assessment of the Impact of Hurricanes Ian and Nicole: Natural and Armored Dunes in the Aftermath of Hurricanes on Florida's Central East Coast. *Remote Sens.* **2024**, *16*, 1557. [CrossRef]

Disclaimer/Publisher's Note: The statements, opinions and data contained in all publications are solely those of the individual author(s) and contributor(s) and not of MDPI and/or the editor(s). MDPI and/or the editor(s) disclaim responsibility for any injury to people or property resulting from any ideas, methods, instructions or products referred to in the content.